Photochemical Internalization of Chitosan/pDNA Nanoparticles

Sigmund Østtveit Størset

December 17, 2010

Preface

This project work was carried through as a collaboration between the Department of Physics, NTNU, and the Department of Radiation Biology, The Norwegian Radium Hospital. The project was done as the course TFY4520 Nanotechnology Project Thesis, giving 15 StP.

I would like to thank Kristian Berg at the Norwegian Radium Hospital for giving me the opportunity of working with the technique of photochemical internalization and for being my supervisor throughout the project. I would also like to thank Catharina de Lange Davies for being my supervisor at the Department of Physics, for helping me with putting up the aims of the project as it went along and for important help and aid during the writing process. I am also grateful for all the help and sincere interest from Sabina Strand.

I would further like to thank Monika Håkenstad from PCI Biotech for teaching me the technique of PCI and the methods involved. Also, Kristin Grendstad Sæterbø deserves great thanks for her invaluable day to day help and patient teaching in the laboratory.

Lastly I would like to thank Nina Kristine Reitan for her help with preparation of polyplexes, and Gøril Flatberg for help with analyzing my flow cytometry data during my last weeks of the project.

Sigmund Østtveit Størset

Trondeim, December 17, 2010

Abstract

Gene therapy is a promising technique for treatment of gene related diseases, but for the technique to be effective and safe, reliable gene delivery systems have to be developed. Chitosan has over the last years been studied intensively as a promising non-viral vector for gene delivery purposes. As a cationic polysaccharide it self assembles with DNA in solution to nanoparticles in the size range of 100nm, which is suitable for transfection of cells. By combining photochemical internalization (PCI), a technique which enhances endosomal release by introducing photochemical damage to the vesicle membrane as a response of activation by light, with gene therapy, increased transfection rates were hoped to be achieved. Also information on mechanisms involved in the transfection process was hoped to be obtained.

Two different chitosan vectors were used: linear chitosan (molecular weight 8kDa, degree of polymerization: 31, degree of acetylation: 0) and self-branched glycosilated and trisaccharide substituted chitosan oligomers (two different types, SBTCO31: molecular weight 27kDa, SBTCO42: molecular weight 27kDa, both substituted with 8.2% AAM and 0 degree of acetylation). The plasmid used for transfection was pEGFP, and complexation was done in a 1:1 hypertonic optiMEM-H_20 solution. The transfection was done in HeLa cells. Illumination for PCI treatment was done with visible light in the wavelength range 400-450 nm with a maximum at 435 nm and an irradiance of 11 mW/cm2. The cells were exposed to light for up to 120s using the photosensitizer $TPCS_{2a}$. Analysis was done with flow cytometry and MTT assay.

The PCI treatment resulted in increased transfection rates using both types of chitosan vectors. For the linear chitosan vector, the rate of transfection increased from $\sim$1% without illumination to $\sim$50% at 120s of illumination, which is equivalent with a 50-fold increase in the transfection rate. Transfection rates using the SBTCO vectors were more than doubled for illumination times of 60s compared to 0s of illumination. High illumination doses also resulted in very high toxicities, especially for transfection using the SBTCO vectors.

The increased transfection rates achieved using PCI treatment reveals that endosomal release is one of the big bottlenecks of transfection using chitosan/DNA nanoparticles. The evident effect of PCI on transfection also proves that PCI in combination with chitosan/DNA nanoparticles is a good approach for effective and cite-specific gene therapy.

Contents

List of abbreviations

A/P	Amine to phospate groups ratio
AAM	GlcNAc-GlcNAc-2,5 anhydromannose
DMSO	Dimethyl sulfoxide
DP	Degree of polymerization
EDTA	Ethylenediaminetetraacetic acid
EGFP	Enhanced green fluorescent protein
F_A	Degree of acetylation
FBS	Fetale bovine serum
FCM	Flow cytometry
FSC	Forward scatter
FWHM	Full width at half maximum
GFP	Green fluorescent protein
GlcNAc	N-acetyl-glucosamine
HEPES	4-(2-hydroxyethyl)-1-piperazineethanesulfonic acid
ISC	Intersystem crossing
MTT	3-(4,5-Dimethylthiazol-2-yl)-2,5-diphenyltetrazolium bromide
PBS	Phosphate buffered saline
PCI	Photochemical internalization
pDNA	Plasmid DNA
PDT	Photodynamic therapy
PI	Propidium iodide
PLL	Poly-L-lysine
SBTCO	Self-branched and trisaccharide substituted chitosan oligomer
SSC	Side scatter
TCO	Trisaccharide substituted chitosan oligomer
ToF	Time of flight
$TPCS_{2a}$	Meso-tetraphenyl chlorin disulphonate
$TPPS_{2a}$	Meso-tetraphenyl porphyrin disulphonate
wtGFP	Wild type green fluorescent protein

1 Introduction

Gene therapy is a promising technique for treatment of gene related diseases. However, for the technique to become a reliable method for bedside medicine, safe and effective gene delivery systems have to be developed. The early trials with viral vectors for gene delivery have by now more or less been totally abandoned due to safety concerns involved in introducing virus particles into the human body [1]. Research have instead focused on non-viral delivery systems, mainly based on polycationic polymers or lipids.

Chitosan has been studied intensely over the last years as a possible non-viral vector for gene delivery. It is a cationic polysaccharide which self assembles in solution with DNA to form chitosan/DNA nanoparticles. Chitosan has proved able to transfect cells both *in vivo* and *in vitro* [2], but there are still challenges to understanding the mechanism of transfection. To be able to develop even more effective vectors, knowledge of intracellular trafficking is crucial, which today still appears as a "black box". Little is known about the mechanisms of the involved processes and especially the mechanism for endosomal release is unclear. Also, which of the processes that stands out as the bottleneck of transfection is unknown.

Photochemical internalization (PCI) is a technique utilizing so called photosensitizers to enhance release from endocytic vesicles by introducing light induced damage to the vesicle membranes. The photosensitizer, which is embedded in the membrane of endocytic vesicles, will when illuminated with visible light make the vesicles to rupture, releasing their contents into the cytosol of the cell [3]. PCI is also a highly site-specific technique because of its dependence of light activation.

The purpose of this study was to use the PCI technique in combination with transfection experiments with chitosan/DNA nanoparticles. This would hopefully give increased cell transfection rates compared to earlier studies. The results could also increase the understanding of whether endosomal release is a bottleneck of the transfection process. Generally, PCI used in gene therapy can hopefully become a powerful tool for achieving effective and site-specific gene therapy treatment of disease.

2 Theory

2.1 Gene Therapy

Gene therapy is defined as the *treatment of a disease caused by malfunction of a gene, by stably transfecting the cells of the organism with the normal gene* [4]. As stated in the definition, the general goal of gene therapy is to alter the overall activity of a cell by influencing its gene expression. This is an approach for curing diseased cells which stands in contrast to simply killing or removing the cells, which often is the standard approach in cancer, which is a genetic disease. In other genetic diseases, killing the diseased cells might not be an option, due to location of the cells (e.g. cells of the brain or central nervous system) or the cells vital function (e.g. that the cells constitute a vital part of an organ). In cases like these, the ability of altering or changing the gene expression of the diseased cells through local influence by gene therapy might be an important contribution on the way to curing the individual from the disease.

The goal of gene therapy is to help cure genetic diseases. This can be done in several ways. In cancer, it can be essential to activate or silence a specific gene to stop the cell from uncontrolled proliferation. It can also be a possibility to introduce a wild type gene which works dominantly over the native gene because the native gene is mutated and does not work properly. Also, a specific gene product, a protein, can be desirable inside the cell, either to introduce cytotoxicity or because the protein's function is desirable itself.

Either way gene therapy consists in introducing DNA material into the cell nucleus of a mammalian cell. This has been a research issue for nearly 30 years [5] and still has many challenges to it. The DNA has to pass through the blood vessel wall and migrate through the extra cellular matrix just to reach the cell. Once there, the DNA further needs to be taken up by the cell or in other ways pass through the plasma membrane to reach cytosol, from where it has to migrate intracellularly to the cell nucleus membrane. Lastly, this barrier has to be passed to get to the cells genome where the DNA can be transcribed. To achieve all this, a method of transportation is needed, which both protects the DNA from degradation, and enhances transportation to and uptake of the DNA into the cell.

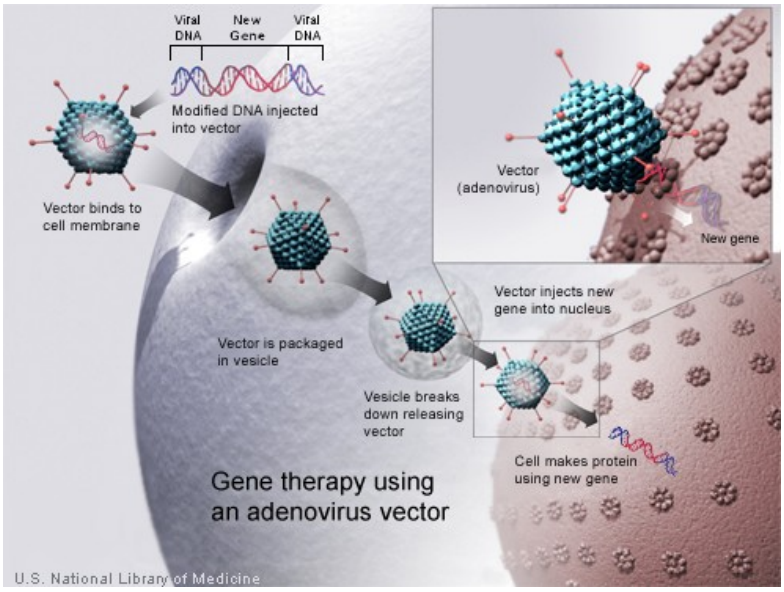

Figure 1: Schematic drawing of gene therapy using a viral vector. If the treatment is successful, the plamid DNA will be incorporated into the genome of the human cell where it will make its protein product [8].

2.1.1 Viral vectors for gene therapy

As naked DNA is taken up by the cell to a very small extent, researchers started looking for vectors that could help DNA over the cell membrane barrier. The first methods used in gene therapy experiments involved viruses as carriers, or vectors, of the desired DNA (see figure 1). These resulted in high transfection efficiencies by utilizing the virus's own mechanism for stable integration of plasmid DNA (pDNA) into the host cell's chromosomal DNA [6]. Even though the high efficiency has been promising, the method involves large safety concerns because of risk of spreading of the virus to other unintended parts of the body [1], and have even lead to a patient's death in one trial experiment in 2007 [7]. Because of this, researchers started looking for other alternatives.

2.1.2 Non-viral vectors for gene therapy

Non-viral vectors are designed to form complexes with DNA such that the vector-DNA complex can be taken up by the cell. Mechanisms for complex

uptake are many, but are probably dominated by endocytosis. This is followed by release from vesicles and intracellular trafficking towards the cell nucleus. The DNA is released from the complex somewhere in the process between uptake and arrival in the nucleus. When in the nucleus, the DNA is not inserted into the chromosomal DNA, but stays in an unintegrated form in the nucleus [6].

The non-viral vectors may be based on polymers (polyplexes) and liposomes (lipoplexes), most commonly, but can also be based on lipid and polymers (lipopolyplex) or peptides or proteins (peptide based) [5]. Polymeric vectors are usually cationic, and by this they form complexes in the nano size regime duo to the negatively charged phosphate groups on DNA. Polyplexes usually contain 3 or 4 pDNA molecules and are rod or toroid shaped. Lipoplexes differ from polyplexes in that they are larger (200-300 nm) and form quasi-spherical vesicles containing only one pDNA molecule [9].

In addition to being less hazardous to the patient, other benefits of non-viral vectors in preference to viral vectors have in the later years been accepted. Non-viral vectors are in general easy and cheap to produce in large scale since they are based on biomaterials as polymers or lipids. Also, since they do not rely on viruses which have their own preferred mechanism of uptake, non-viral vectors are easier to conjugate for specific targeting [10].

2.2 DNA-vector complex internalization

Clathrin-dependent endocytosis was for a long time considered the only mechanism capable of taking up lipo- and polyplexes into the cell [9]. It is now clear that also other pathways, so called clathrin-independent endocytosis, also are important for polyplex and lipoplex internalization [11]. Suggested mechanisms include phagocytosis and macropinocytosis, but especially caveolin-dependent endocytosis is believed to be important [11, 12]. The vesicles resulting from this kind of uptake are believed to end in the cavoesome. The faith of this organelle is highly discussed, but it is believed that it merges with the early endosome [13, 14]. An important difference between the endosome and the caveosome is that the latter has a neutral pH, whereas the endosome has an acidic pH level, which activates numerous enzymes important for endosomal degradation [14]. By this, lipoplexes and polyplexes taken up through clathrin-dependent endocytosis are at a much higher risk of degradation than complexes taken up through the caveolin-

dependent endocytosis.

2.3 Chitin and chitosan

Chitin is a biopolymer consistent of N-Acetylglucosamine monomers. This monomer is related to glucose, which is the monomer of cellulose. Chitin, as cellulose, is abundantly found in nature in the outer skeleton of shrimps, crabs and related animals [15]. Chitosan is formed by partially deacetylation of chitin (more than 60% deacetylated monomers). This gives chitosan a positive charge because of protonation of the free amino groups resulting from the deacetylation process. The result is a cationic, biodegradable biopolymer, as seen in figure 2.

The last 15 years experiments have been done with chitosan as a non-viral and non-synthetic vector for gene therapy. In addition to being biodegradable, it has been found non-cytotoxic and non-immunogenic [16]. All chitosans form polyplexes with DNA, but the stability of the complexes depend strongly on the degree of acetylation (F_A, percent of monomers which are acetylated) of the chitosan, where fewer acetyl units give more stable complexes. Also, the pH of the complex solution and the chitosan amine group to DNA phosphate groups ratio (A/P ratio) are important factors for complex formation and stability [19]. Polyplex stability is reduced when the pH value exceeds 7.4. This is because the amino groups of the chitosan chains to a high extent are deprotonated above this pH, and by this the chitosan loses its positive charge. The length of the chitosan oligomer chain also strongly influences the stability and transfection ability of the polyplexes [17]. A too short chain will not bind DNA sufficiently and give unstable polyplexes. A too long chain on the other hand will bind DNA too strongly which reduces the release of DNA to cytosol and the cell nucleus which gives a overall reduced gene transcription. Studies have shown that the stability and unpacking properties of the polyplex is best balanced at an oligomer chain length of between 30 and 40 monomer units [17].

2.3.1 Linear chitosan

Linear chitosans consist of independent chains of N-Acetylglucosamine, which are deacetylated to a certain extent and has a certain degree of polymerization (DP, average number of monomers in one oligomer). It was these types of chitosans that first were used as vectors for gene therapy. However, al-

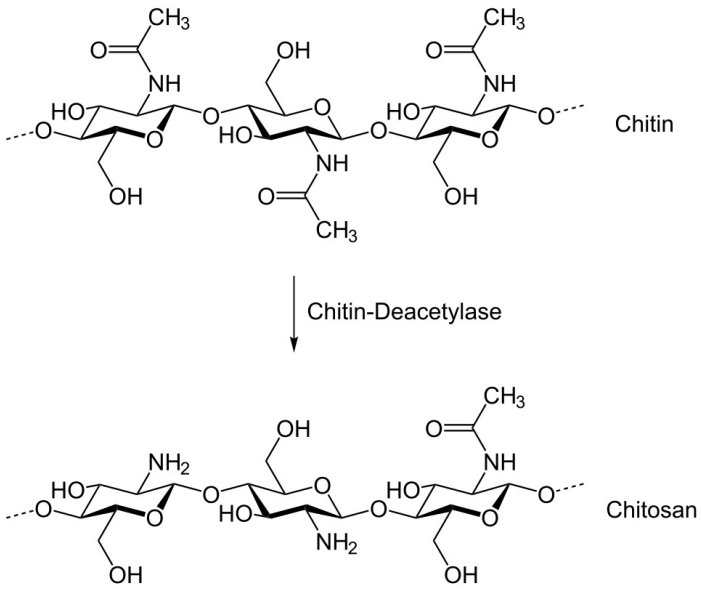

Figure 2: The figure shows three monomer units of both chitin (top) and chitosan (bottom). Deacetylation of a chitin oligomer to a degree of more than 60% gives chitosan [18].

though chitosan was early believed to be a good DNA vector, the linear chitosan's capacity of delivering genes to cells at physiological pH has not met the expectations [20].

2.3.2 Self-branched glycosilated (trisaccharide substituted) chitosan oligomers

Lectins are known to bind sugar residues. When lectins sitting in the cell membrane bind to its ligand, the ligands are internalized in a vesicle and delivered to an early endosome. This has been utilized to achieve higher transfection efficiencies of chitosan vectors [21]. By substituting the trisaccharide GlcNAc-GlcNAc-2,5 anhydromannose (AAM) to the primary amines in the chitosan chain, a vector with a 4-fold higher transfection efficiency than the linear chitosans has been achieved. These new trisaccharide substituted chitosan oligomers (TCO) were also shown to aggregate less than the linear chitosans [21].

To further increase the stability and efficiency of the chitosan vectors, a

self-branched and trisaccharide substituted chitosan oligomer (SBTCO) has been developed [20]. Here, the different AAM-substituted oligomers are linked together through a self-branching step which involves Schiff base formation between two monomers of different oligomers. The SBTCO vectors have proved able to reach a transfection efficiency up to 70% in HEK293 cells [20].

2.4 Photodynamic Therapy

Photodynamic therapy (PDT) refers to the technique where a photosensitizing agent (a photosensitizer), often tumor localizing, absorbs in the plasma membrane of a cell and causes fatal photochemical damage to the cell when activated by light in the visible spectrum [22]. This effect was discovered as early as 1900 when it was noticed that the photosensitizer acridine in the presence of light was able to kill paramecia [23]. Present day photosensitizers, mostly porphyrins, has a preferred uptake and accumulation in tumor tissue [24]. The photosensitizers are usually amphiphilic, which makes them absorb in the outer part of the plasma membrane with its hydrophobic part inside the lipid layer of the membrane, and its hydrophilic part sticking out of the membrane outside the cell.

PDT is a two stage treatment approach. In the first stage, the photosensitizer is added to the cells which are to be treated. In the second stage, light is applied directly on the region where the toxic effect of PDT is desired. Upon illumination, the photosensitizer is excited to its first or higher energy level. The lifetime of the higher states are very short (picoseconds), whereas the first excited state has a somewhat longer lifetime (nanoseconds). From this state, intersystem crossing (ISC) can occur because of the system of conjugated π bonds in the macrocyclic photosensitizer. This triplet state of the photosensitizer can react in two ways, through a type I or a type II mechanism (see figure 3). The type I reaction involves transfer of electrons or protons, creating radicals and reactive oxygen species. Type 2 reactions create singlet oxygen ($^1 0_2$) [25].

The singlet oxygen species is highly cytotoxic, and has short lifetime in a liquid environment (< 40ns). Because of this, the species will not be able to migrate far, and therefore has a short radius of action, less than 20 nm [22]. This gives PDT a very local effect. The cytotoxic effect of $^1 0_2$ is mainly because of membrane damage caused by oxidation of amino acids [3]. This can give direct cell killing, vascular damage or immune responses.

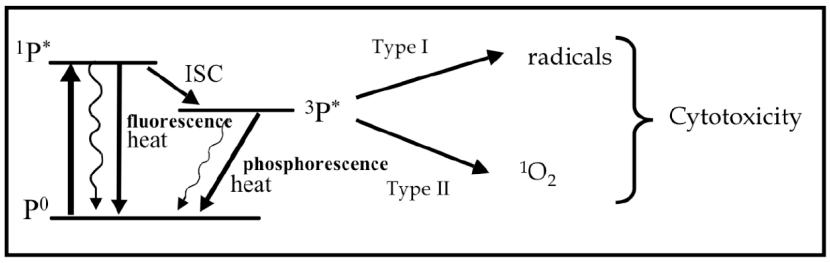

Figure 3: A Jablonski diagram of the basic mechanism of PDT is shown on the left side (vibrational levels are not shown). Due to allowed intersystem crossing (ISC), the triplet state of the photosensitizer will be present when excited. This state of the molecule reacts and gives cytotoxic radicals (type I reaction) or $^1 0_2$ (type II reaction) [3].

2.5 Photocemical internalization

The major difference between PDT and PCI is that the latter technique activates photosensitizers which mainly are situated in the membrane of endocytic vesicles. Photosensitizer activation by light is followed by endocytic vesicle membrane rupture, which gives release of the contents of the vesicle [26]. When a vesicle bulges of the plasma membrane for endocytic uptake into the cell, photosensitizers which are absorbed in the membrane will follow in the process and thus end up on the inner side of the vesicle membrane (see figure 4). If the goal of the treatment is to kill the cells using a drug, light can be applied directly to release the contents of the vesicles and induce the cytotoxic effect of PDT. If, on the other hand, the goal of the treatment is to effectively introduce a macromolecule into cytosol without inducing any cytotoxic effect (as for gene therapy), the cells can be washed repeatedly before illumination. By this, photosensitizer absorbed in the plasma membrane will be washed away and reduced in numbers before light is applied, and thus reduce the cytotoxic effect of PDT. In an *in vivo* experiment, the washing procedure is taken care of by the flow of extracellular fluid.

When a culture of cells is treated with PCI to enhance transfection in gene therapy, a portion of the cells will die due to the toxic effect caused by the excitation of the photosensitizer. A long illumination time creates more $^1 0_2$, and will therefore give a higher toxic effect. A good PCI treatment protocol sets the time of illumination such that a good balance between $^1 0_2$ in endocytic vesicles and the plasma membrane is obtained. By this, en-

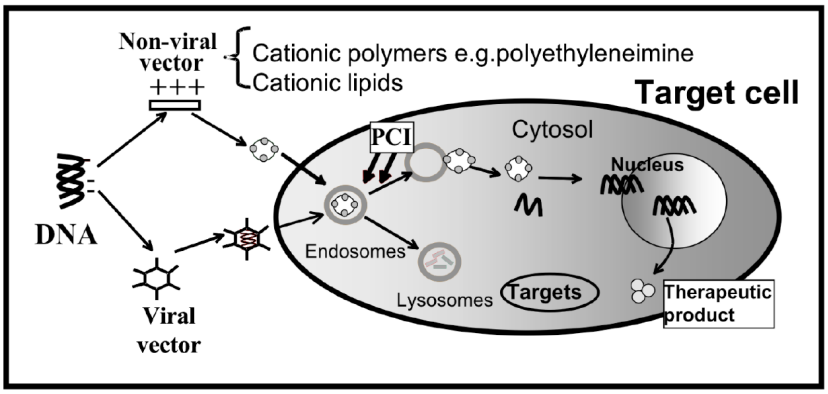

Figure 4: The role of PCI in gene therapy. The pDNA is carried over the plasma membrane barrier either as part of a complex with a non-viral vector or as part of a viral vector. Once inside the endosome, the DNA/vector complex can either be released or degraded in the lysosome. Alternatively, PCI stimulates the release of the complexes, and the pDNA can reach the nucleus and the gene product can be expressed [3].

hanced endosomal release can be a achieved without enhanced cell killing (due to the washing step in the procedure which gives a higher abundance of photosensitizer in endosomal vesicles than in the plasma membrane).

2.5.1 The $TPPS_{2a}$ and $TPCS_{2a}$ photosensitizers

Two photosensitizers often utilized for PCI are meso-tetraphenyl chlorin disulphonate ($TPCS_{2a}$) and meso-tetraphenyl porphyrin disulphonate ($TPPS_{2a}$). They differ only by one double bond in the pyrrole ring of the molecule on the hydrophilic side, as seen in figure 5 [27]. Both photosensitizers are amphiphilic by substitution of two sulphonate groups on one side of the molecules. $TPPS_{2a}$ is a phorphyrin, as many other photosensitizers, while because of the one missing double bond, $TPCS_{2a}$ is porphyrin related. Both photosensitizers have absorption maxima in the blue region of visible light, around 415nm, varying with different solvents [27]. Emission maxima are at around 650 nm for $TPPS_{2a}$, and slightly higher for $TPCS_{2a}$, at 655 nm. The absorption spectrum of a typical porphyrin type photosensitizer is seen in figure 6. Both $TPPS_{2a}$ and $TPCS_{2a}$ are known to produce $^1 0_2$ after excitation. This causes the toxic effect which makes the endocytic vesicles rupture. $TPPS_{2a}$ gives a higher $^1 0_2$ yield than $TPCS_{2a}$ when excited at their relative

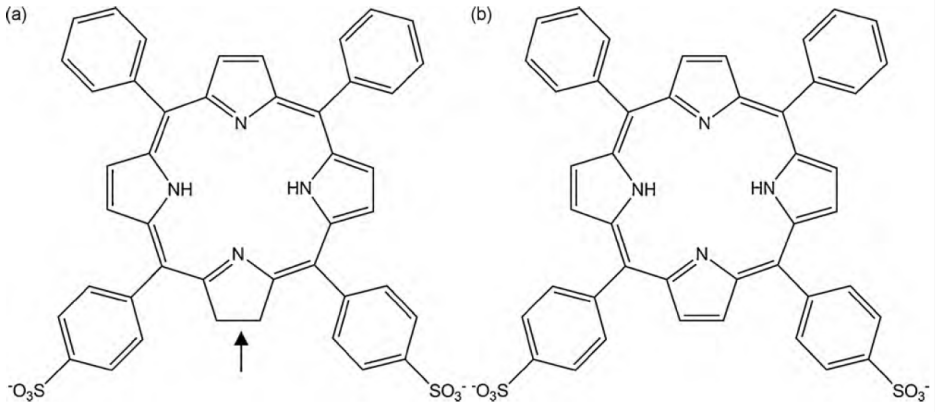

Figure 5: Structural formulas of the photosensitizers $TPCS_{2a}$ (a) and $TPPS_{2a}$ (b). The only difference is the missing double bond in $TPCS_{2a}$, which is indicated by the arrow. $TPPS_{2a}$ is a porphyrin while $TPCS_{2a}$ is porphyrin-related. [27].

absorption maxima [27].

2.6 Toxicity, viability and transfection analysis

To find a good illumination time for PCI in an experiment series, it is necessary to measure both survival and transfection rates of the cells.

2.6.1 Viability analysis with MTT

An MTT assay is used to give a quantitative measure of the viability of living cells. 3-(4,5-Dimethylthiazol-2-yl)-2,5-diphenyltetrazolium bromide (MTT) is reduced to a purple farmazan in active mitochondria in living cells [28]. The produced farmazan is in crystal form, and has to be dissolved using a solvent as HCl or dimethyl sulfoxide (DMSO). After dissolution, the absorbance of the cell culture sample can be read on a multiwell spectrophotometer and compared to other samples or blank wells. The MTT assay is a quick and versatile method for measuring cell viability, which can be interpolated to data on cytotoxicity in comparable samples. Since the method relies on active mitochondria, a reduction in cell activity gives the same result as a reduction of the number of living cells.

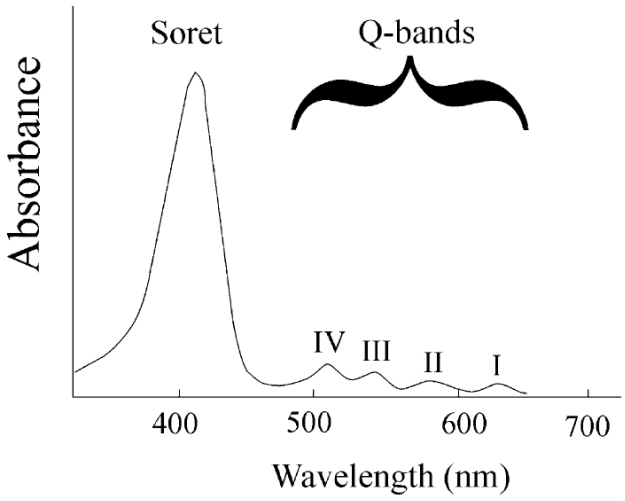

Figure 6: The absorption spectrum of a typical porphyrin type photosensitizer. Typically, it has one absorption maximum around 400nm (Soret-band) and several minor absorption maxima at longer wavelengths (Q-bands) [25].

2.6.2 Toxicity measurements with propidium iodide

When cells die, either through apoptosis or necrosis, their plasma and nuclear membranes get leaky and allows for diffusion of molecules to and from cytosol and the nucleus. Propidium iodide (PI) is a small molecule of molecular mass of 668.4 Da, which binds DNA through intercalating between bases [29]. It binds randomly with one PI molecule for every four to five bases. When excited by a 488nm laser, PI fluoresces with maximum at around 617 nm.

When PI is added to cell sample, PI will be able to diffuse through the permeable membranes of dead cells followed by DNA binding. Flow cytometry analysis (see section 2.7) of the sample can then give a quantitative measure of number of dead cells because only DNA of dead cells will be stained with PI.

2.6.3 Transfection measurements with EGFP

Green fluorescent protein (GFP) is a protein of 26,9 kDa, which fluoresces at 508 or 503 nm (bright green) when excited at its major excitation peak at 395 nm or at its minor peak at 475 nm respectively [30]. GFP was first discovered in 1962 by Shimomura et al. in Aequorea jellyfish [31], but it was

not until 1990 experiments relevant for gene therapy were carried out. Since GFP folded and was fluorescent at room temperature and at 37^oC it was a very good candidate as a marker for transfection. It is now widely used for this in fields as gene therapy.

Wild type GFP (wtGFP) has several drawbacks as a transfection marker, including sensitivity, poor intensity when excited at its minor peak (blue light, 475nm), and poor expression in several mammalian cell types. To improve the properties of wtGFP, Zhang et al. [32] constructed a GFP variant with chromophore mutations to achieve 35 times higher fluorescent intensity. It was also codon-optimized for higher expression in mammalian cells. This GFP variant is called enhanced green fluorescent protein (EGFP).

Even though EGFP has become a standard transfection marker in cell transfection experiments, it has been reported toxic to cells when incubated over a longer time period (several days) [33].

2.7 Flow Cytometry

Flow cytometry (FCM) is a quantitative technique for analyzing cells and other microscopic particles [34]. It utilizes a jet stream which arranges the cells from the sample into a line, and passes them by an electronic detection device one by one. In this detection device, information on the cell's chemical and physical properties can be detected by use of both scattering and fluorescence information. If the sample (e.g. cellular) is properly stained, there will be a proportionality between the intensity of fluorescence from the cell and the cellular parameter which is stained. By this, it can be possible to divide the cells in the sample into different groups, e.g. cells with high and low DNA contents (which would correspond to dividing and non-dividing cells).

2.7.1 Basic principles

The sample which is to be analyzed has to be in liquid form. It is injected into a flow cell where a sheath fluid surrounding the sample inlet forces the sample fluid into a thin stream where the cells/particles are organized into a line (hydrodynamical focusing, laminar flow). A bright laser is directed onto the stream of fluid, surrounded by several detectors. Two detectors measure intensity of scattered light, whereas one or more detectors measure fluorescence from fluorescent dyes inside or on the surface of the cells/particles. Figure 7 gives a schematic representation of the flow cytometer setup.

The detectors for scattered light are the forward scatter (FSC) detector and the side scatter (SSC) detector. The forward scatter detects low angle scattering (0.5 to a few degrees, the direct beam is blocked) when a cell/particle passes through the beam of light. This gives information on the size of the cell/particle. The side scatter gives a measure on the amount of highly scattered and refracted light (at $\sim 90^o$), and gives information on the internal structure and surface texture of the cell/particle. Early apoptotic cells will often have a high SSC signal because of changed morphology, and can also have an decreased FSC signal because of reduced size (proportional relation). A cell containing large amounts of organelles and vesicles will give an increased SSC signal because of increased scattering from the internal structures of the cell.

The FSC and SSC signal can be detected either as the integral of the total signal or as the time of flight (ToF). The time of flight is the time the cell/particle uses to pass the laser beam and is measured as the full width at half maximum (FWHM).

The fluorescent detectors measure fluorescence intensity from different fluorescent dyes which have been used to mark specific details in the sample. Excitation with several lasers of different wavelengths is possible, as long as the emission spectra of the dyes are not overlapping significantly. Saturation of the fluorescent detectors from the excitation laser light is avoided by using filters in the detectors such that only the emission maximum from one dye affects one detector.

The best flow cytometers can now collect information from a sample at a speed of up 75.000 cells/particles per second. When several fluorescent dyes are used in combination with information from the FSC and SSC detectors, precise information on several different parameters can be collected from each single cell/particle at a very high speed compared to other cell analysis techniques.

2.7.2 Data analysis

Data from a flow cytometer run can be presented in a histogram or to dimensional dot plot. Three dimensional plots are also available in some softwares, but are less used. The axes on flow cytometer plots are often logarithmic since fluorescent and scattering intensity has a large range. Because of noise and overlap of different dye emission spectra, each detector has to be gated so that a signal weaker than a certain limit value will not be part of the

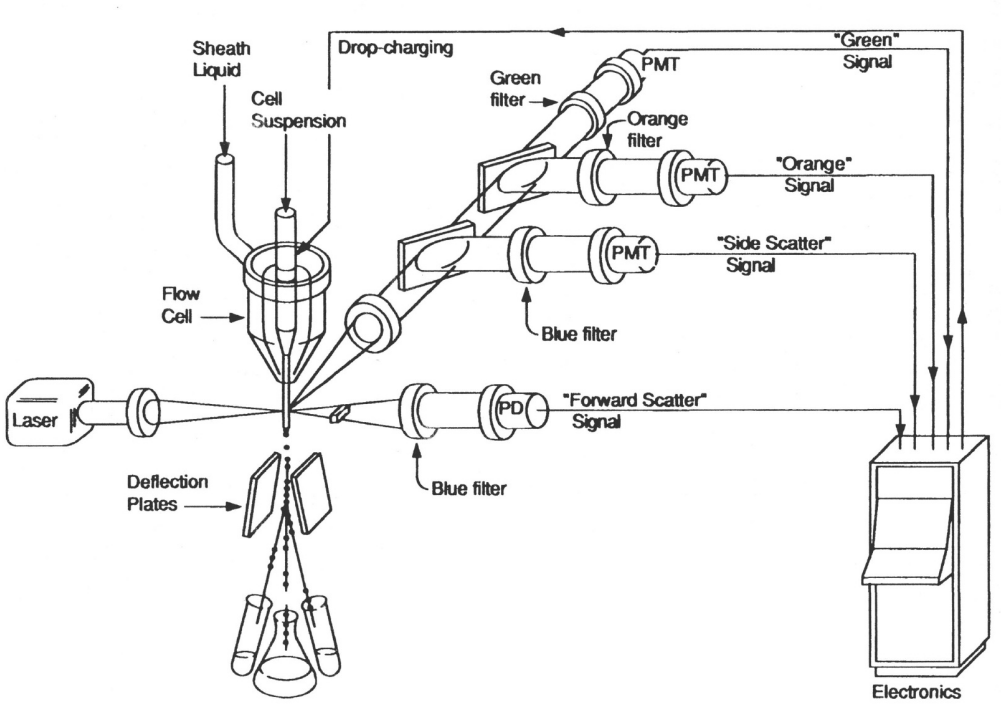

Figure 7: Schematic representation of flow cytometry. A laser is directed onto a flow of single cells. Detectors for forward scattering, side scattering and fluorescence at different wavelengths surround the intersection of the stream of cells and the laser. [35].

statistics or not detected at all.

Single dimension plots, giving histograms, represent counts (y-axis) versus light intensity of one detector (x-axis). This is a good way of representing data for e.g. amount of an organelle or protein (stained with a fluorescent dye) inside each cell. In a two dimensional plot, two detectors are plotted against each other (one at each axis) and each cell/particle is marked with a dot. This is a good way of representing data when separation of subspecies of different sizes or morphology within the sample is desired. Clusters of dead versus viable cells can for example be seen in this representation.

3 Materials and methods

3.1 Materials

3.1.1 Cell lines

HCT116 cells (human corectal carcinoma cells, LGC Standards-ATCC) were used for the initial experiments and technique establishment. HeLa cells (human cervical carcinoma cells) were used for all experiments with chitosans as transfection vector.

3.1.2 Cell cultivation reagents

Both HCT116 cells and HeLa cells were cultured in T_{175} flasks (nunc). HCT116 cells were added 20 mL of RPMI-1640 medium (Sigma-Aldrich), which was added 10% fetal calf serum (FBS, Gibco BRL), 100 U/mL penicillin, 100 μg/mL streptomycin and 2mM glutamine (all reagents from Sigma).

HeLa cells were added 20 mL of Dulbecco's Modified Eagle Medium (DMEM,Gibco Invitrogen), which was added 10% FBS, 1% non-essential amino acids (NEAA, Gibco Invitrogen) and 0.5% L-glutamin (200mM, Sigma Aldrich).

For splitting of the cells, trypsin/edta solution (0,25 %/0,02%, Sigma-Aldrich) and phosphate-buffered saline (PBS, 1x, Sigma Aldrich) was used. Both reagents and media described above were stored at $+4^oC$.

When it in section 3.2 Methods refers to medium, this does always mean the medium mixtures described above.

3.1.3 The photosensitizer

The photosensitizer $TPCS_2a$ was used in all experiments. It was produced by Synthetica. Stock concentration was 0.35mg/mL with Cremophor (BASF SE) as solvent. It was stored dark at $+4^oC$.

3.1.4 EGFP pDNA

EGFP pDNA was prepared using the NucleoBond Xtra Midi kit (Macherey-Nagel). The final concentration of EGFP pDNA was measured to 1,58 μg/mL using absorbance analysis. Full protocol for pDNA preparation can be found in Appendix A.

3.1.5 Complexation vectors

Poly-L-Lysine Poly-L-Lysene HBr (PLL, MW 15-30 kDa, Sigma) was used as vector for PCI experiments with HCT116 cells. The PLL was dissolved in distilled water to a concentration of 1μg/mL. The solution was sterilized by filtration and stored at -20^{o}C.

Chitosan Different chitosans were used as vectors for PCI experiments with HeLa cells. Both linear chitosans and SBTCOs were produced at NTNU by Sabina Strand's group. The linear chitosan had molecular weight 8kDa and degree of polymerization of 31. Two different SBTCO chitosans were used. SBTCO31 had a molecular weight of 20kDa, while SBTCO42 had a molecular weight of 27kDa. Both SBTCOs were substituted with 8.2% AAM (mole percentage compared to number of deacetyleted units, GlcN). All three chitosans were 100% deacetylated, that is $F_A = 0$.

All chitosans were stored in stock solutions of 2.0μg/mL at -20^{o}C.

3.1.6 MTT

MTT (Sigma) was dissolved in PBS to a stock concentration of 5mg/mL, sterilized by filtration and stored dark at +4^{o}C. 100% DMSO (Sigma-Aldrich) was used to dissolve the farmazan crystals.

3.2 Methods

All reagents which were to be added to cells in larger amounts were preheated to 37^{o}C in a water bath. This did not include chemicals which were added to larger solutions in small volumes.

Inspection of the cells during experiments when appropriate was done with a phase contrast transmission microscope (Leica DMIL) with objectives of 10X and 20X.

3.2.1 Cell cultivation

Both HCT116 cells and HeLa cells were split twice a week, usually Mondays and Thursdays. The growth medium was sucked away followed by washing with 5mL PBS. After removing the PBS, 3mL of trypsin was added to the flask to make sure that the whole flask surface was wetted. 2mL of the added trypsin was removed before incubation at 37^{o}C and 5% volume to volume

(v/v) CO_2 for 5-10 minutes, until all cells had loosened. After incubation the cells were resuspended in 10mL medium in a 15mL centrifuge tube. Using a 5mL Pasteur pipette, some droplets of the cell suspension were added to a Burker chamber. The cells were centrifuged at 1500rpm for 5minutes and the medium with trypsin was discarded. Using the transmission light microscope, the cells in the counting chamber were counted to decide the cell concentration. From this, the cells were resuspended in fresh medium to the desired final concentration. For both cell lines a total of $2{\cdot}10^6$ cells were added to the new T_{175} flask. This corresponds approximately to a 1:20 splitting for HCT116 cells and to a 1:8 splitting for HeLa cells.

3.2.2 Treatment of cells

A PCI experiment has the general protocol described below. For each set of experiments, parallel samples for MTT and flow cytometry were prepared. Each setup had samples which were treated with different light doses and samples without complexes to look at the general toxicity of the photosensitizer (PDT samples). A number of negative controls which did not get any light treatment were also made. These negative controls were:

- No treatment (NT): only medium added in each step described below.
- No light (NL): only photosensitizer added, but not complexes.
- Complexes: only complexes added, but not photosensitizer.
- Complexes, no light: both complexes and photosensitizer added.

Samples were produced in duplicates for FCM and triplicates for MTT.

All work with cells were done in a sterile environment. In the protocol below, this involves work on day 1 and 2, but not on day 4 since these cells not were to be cultivated any longer. All reagents which were to be added to cells during sterile work were sterilized by filtration.

Day 1 Cells in their respective growth medium were seeded into wells on 96 wells plates (MTT) or 24 wells plates (FCM) (Corning Incorporated). The cell concentration was 65.000 cells/mL. For MTT 0.1mL cell solution was added per well, and for flow cytometry 0.5mL solution was added per well. This was followed with incubation at 37^{o}C and 5% v/v CO_2 for 18 hours

for HCT116 cells or ∼6 hours for HeLa cells, until the cells had attached to the wells. The following protocol is valid for HeLa cells, since the longer incubation time in this first step adds one extra day to the protocol. The protocols for the two cell lines are otherwise alike.

After incubation fresh medium with 0.2μg/mL photosensitizer (0.1 mL for MTT, 0.5 mL for FCM) was added to each well followed by incubation for 18 hours (37^{o}C, 5% v/v CO_2).

All work done with samples after day 1 in the experiment protocol had to be carried out in a dark environment, since most samples contained photosensitizer. If work had been done in a light environment, it would lead to extensive cell death due to the toxic effect of the excited photosensitizer. The work did not need to be carried through in total darkness, but no direct light should hit the samples, and ceiling lamps should not be turned on in the area of the room where the experiments are carried through.

Day 2 All wells were washed twice with medium before addition of pDNA/ vector complexes. Volumes for both washing and complex addition were as before, 0.1mL for MTT samples and 0.5mL for FCM samples. For preparation of complexes, see section 3.2.3. The cells were incubated for 4 hours (37^{o}C, 5% v/v CO_2), followed by a single wash of each well and addition of fresh medium. Lastly the cells were illuminated with different light doses (see 3.2.4).

Day 4 Two days after illumination (incubated at 37^{o}C, 5% v/v CO_2) the samples were analyzed for expression of EGFP using FCM (see 3.2.5). Cell survival was analyzed through PI staining in FCM and cell viability was analyzed through an MTT assay (see 3.2.6).

3.2.3 Preparation of pDNA-vector complexes

PLL polyplexes PLL polyplexes were prepared with an A/P ratio of 2.2. 2.5μL pDNA (stock solution of 2.0 μg/μL) was diluted with 47.5μL H_2O (DNase, RNase and protease free, 5 PRIME), and 6.92μL PLL (stock solution 1μg/μL) was diluted with 42.08μL H_2O. pDNA and PLL solutions were mixed gently and incubated for 30 minutes at room temperature before dilution to a total volume of 1mL by adding fresh medium. The polyplex

solution was then added to each well, 0.1mL for MTT wells and 0.5mL for FCM wells.

Chitosan polyplexes pDNA chitosan polyplexes were prepared with A/P ratios of both 5 and 10. For an A/P ratio of 10, the amount of chitosan is doubled compared to the amount needed when preparing polyplexes of A/P 5. The extra volume is compensated for by adding less H_2O.

For polyplexes of linear chitosan and A/P ratio 5, 8.42μL pDNA (stock solution 1.58 μg/μL) was added to 972.16μ H_2O (DNase, RNase and protease free, as for PLL polyplexes). While stirring this intensly on a vortex mixer ($\sim$1200 rpm on a MS1 minishaker, IKA laboratory equipment), 19.42μL (stock solution 2μg/μL) chitosan was added dropwise. Incubation for 40 minutes at room temperature with no light exposure followed. For substituted chitosan (SBTCO), the volume of chitosan added was 22.68μL (stock solution 2μg/μL). The protocol was otherwise the same (except for less H_2O because of larger volume of chitosan).

Directly before addition to the cells, the polyplexes were diluted 1:2 with a hypertonic optiMEM solution. This was prepared from 40mL OptiMEM (Gibco Invitrogen) which was added 0.1904g HEPES (Sigma) and 1.94g mannitol (AnalaR, BDH). This solution was pH adjusted to 7.0 and sterile filtered before use.

3.2.4 Illumination

The cells were illuminated with a lamp from LumiSource, borrowed from PCI Biotech. The plates containing the samples were placed on a flat window on top of the light source which is designed for uniform exposure. The lamp was delivered with 4 light tubes (4x18W, Osram) which emit blue light in the wavelength range of 400-450nm with a maximum at 435nm and an irradiance of 11mWcm^{-2}. Different light doses could be given to different wells on the same plate by simply moving the plates over the edge of the illumination window.

3.2.5 Measurement of cell transfection

To avoid discarding of dead cell which no longer were attached to the well surface, the medium from each well was removed by pipetting and kept in separate 5mL centrifuge tubes. The cells were then washed with PBS (0.2mL

per well) before trypsination (0.1mL per well, incubation for 5-10 minutes at room temperature). After the cells had loosened, they were resuspended in their old medium containing dead cells and added to new centrifuge tubes through a Cell Strainer Cap filter (DB Falcon, 50μm mesh nylon filter). 10μL PI (Sigma Aldrich, stock solution 50μg/mL) was added to each sample to reach a final concentration of 1μg/mL. Samples were stored dark and on ice until FCM analysis. A total of 10.000 cells were collected from each sample (ungated, containing both living and dead cells). Some samples contained very few cells, and for these the FCM analysis was disrupted after 600s if not 10.000 cells were reached. This resulted in some analysis containing data from as few as $\sim$2000 cells. Data were analyzed using the Kaluza software (Beckman Coulter).

3.2.6 Measurement of cell viability

Fresh medium 0.25 mg/mL MTT was added to each well (0.1mL per well) and incubated between 1 and 3 hours (37^{o}C, 5% v/v CO_2). MTT solution was also added to three empty wells as blank samples for the analysis. The incubation time was dependent on how confluent the cells were and the cells' general viability, which varied somewhat between experiments. After incubation, the MTT solution was removed and the formazan crystals were dissolved in 0.1mL DMSO and put on a Shuttler MTS2 plate stirrer (IKA laboratory equipment) at 300rpm for $\sim$2 minutes. The absorbance from the samples was measured on a SpectraMax Plus384 microplate reader (Molecular Devices) at a wavelength of 570nm.

3.3 Flow cytometry setup

The samples were analyzed in a Gallios flow cytometer (Beckman Coulter) with a blue laser of 488nm. Eight samples were loaded into the sample carousel at a time, the rest were kept on ice. EGFP fluorescence was detected through a 525nm filter with 40nm band pass, while PI fluorescence was detected through a 620nm filter with 30nm band pass. Both SSC and FSC integral and time of flight signals were also detected.

To eliminate aggregates of cells (doublets and triplets etc) from single cells, integral SSC was plotted against time of flight SSC in a linear dot plot. Dead cells were eliminated by plotting linear FSC against logarithmic PI fluorescence. By gating on the regions with viable and single cells from the two

previous plots, a plot of EGFP expressing, singlet and viable cells could be generated. This was plotted as linear SSC against logarithmic EGFP fluorescence. In this plot, a clear population on neagative cells would be present to the left. EGFP positive cells would be defined as cells spread out to the right of this population starting at a preset minimum separation.

A histogram of counts versus logarithmic EGFP fluorescence was also generated. This plot held information on bulk shifts in cell population and broadening if the population in EGFP positive samples. General flow pages from FCM analysis can be seen in Appendix B.

The number and percent of EGFP positive cells were defined as above. To investigate the degree of transfection in the positive cells, the arithmetic mean of each sample was analyzed. A higher arithmetic mean of a sample with the same transfection rate as another, would mean a stronger EGFP fluorescence signal from each cell on average. This gives information on the average degree of transfection per cell in the sample.

Since the emission spectra for EGFP and PI overlap to a certain extent, fluorescence spill from each dye into the other dye's detector had to be compensated for. By creating a EGFP fluorescence versus PI fluorescence logarithmic dot plot, the spill could be investigated. Analyzing a sample only containing EGFP dyes should be compensated such that the plot gives a single vertical line. The vertical line is present because all cells give equal PI fluorescence intensity, which should be zero. Equally, by analyzing a sample only containing PI stained cells, a horizontal line should occur when the sample is compensated properly.

The compensation was decided during the first experiment done with HeLa cells, and found to give best results when the compensation for PI spill in the EGFP detector was $\sim$0.2% and the compensation for the EGFP spill in the PI detector was $\sim$10%. In subsequent experiments, the compensation was adjusted to fit each experiment series best possible, and took values in the region of 0% to 0.5% and 10% to 12% for the two detectors respectively. Examples on comparison of an uncompensated and a compensated dot plot can be seen in Appendix C.

4 Results

4.1 PCI with HCT116 cells and PLL/EGFP polyplexes

During week 35 an educational visit was made to Kristian Berg's group at the Norwegian Radium Hospital. There the technique of PCI was demonstrated, and all methods involved in the technique were gone through. The standard protocol which was utilized in the demonstration used HCT116 cells and PLL as vector. The first goal when starting up experiments at NTNU was to reproduce the results from the Radium Hospital. Because of this, HCT116 cells and PLL-vector were utilized in the first experiments.

Illumination times were set to 120s, 240s, 360s and 480s for the PDT and PCI samples. Figure 8 shows an overlay histogram of three different samples from the experiment: no treatment (blue), complexes (red) and PCI240 (green). The two leftmost histograms (no treatment and complexes) overlap quite significantly, meaning that the PLL/EGFP polyplexes give little to no transfection without PCI treatment. The arithmetic means of these samples were 0,34 (no treatment) and 0.33 (complexes) The rightmost histogram represents the PCI sample which received 240s (4 min) of illumination. The histogram is shifted to the right and has a tail rightwards on the x-axis (EGFP fluorescence axis) and an arithmetic mean of 20.7, which represents over a 60-fold increase in rate of transfection from the complexes sample. This indicates that a number of cells are transfected as a result of the PCI treatment. At the illumination time of 120s, the sample showed a survival rate of 96.8% and a transfection rate of 12.1% (% transfected of living cells). For light doses of 240s, these percentages had changed to 91.8% and 16.2% respectively. For higher light doses too few cells were collected to achieve reliable data (<1000 cells).

The MTT analysis showed that the viability of the cells fell drastically between 120s and 240s of illumination (data not shown). Also, the degree of absorbance was comparable for control samples with and without photosensitizer for both samples with and without polyplexes, meaning that incidental light exposure during experiments did not lead to mentionable cell death and that the presence of polyplexes not lead to mentionable cell death either.

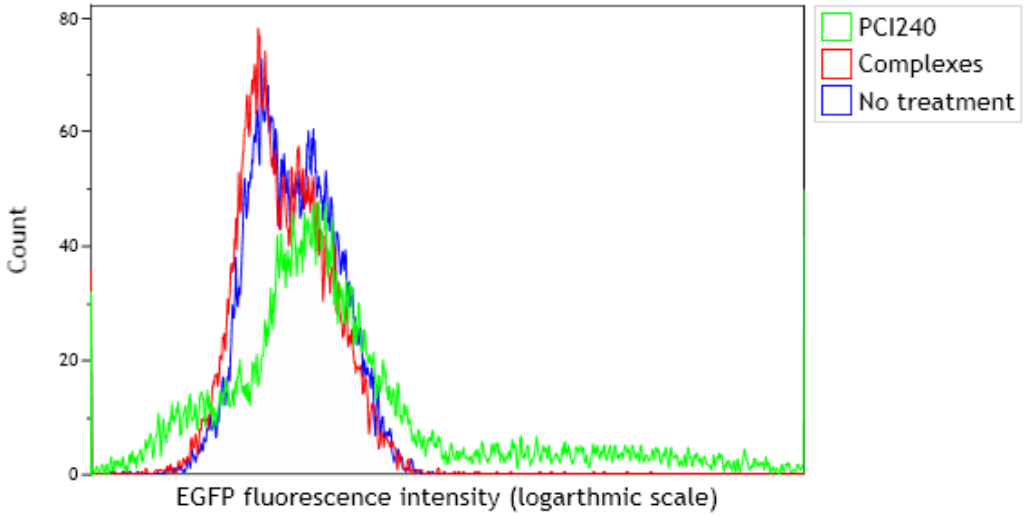

Figure 8: Overlay histogram of three different samples of HCT116 cells with PLL/pDNA polyplexes (counts versus EGFP fluorescence intensity): PCI240 (green), complexes (red) and no treatment (blue). The arithmetic means of the samples were: PCI 240: 20.7, complexes: 0.33 and no treatment: 0.34. All histograms are gated on viable singlet cells.

4.2 Toxicity analysis of $TPCS_{2a}$ with HeLa cells

PDT treatment protocols differ from cell type to cell type. Some cells can handle large amounts of PDT treatment before toxic effects occur, whereas others can handle very little. Before experiments with HeLa cells and chitosan/pDNA polyplexes could be carried through, a PDT illumination protocol had to be determined.

The only parameter which was decided to be changed from the protocol in the former experiment was the illumination time. The concentration of photosensitizer and cells stayed unchanged. The first approach to decide the appropriate light doses was simply inspection with a transmission light microscope after PDT treatment. 0.2μg/mL photosensitizer was added to a T_{175} flask which contained $\sim$3 million cells. After following the protocol with washing and incubation, the flask was divided into eight equally sized regions and illuminated for 0 to 7 minutes. By optical inspection 24 hours after illumination, the cells were estimated to be 100% dense (by definition in this specific experiment) for areas which received 0 and 1 minute of illumi-

nation, 50% dense for 2 minutes of illumination, 20% dense for 3 minutes of illumination, and <5% dense for illumination times of 4 minutes and more. Since it is desirable to achieve an as high transfection as possible with an as low toxic effect a possible in gene therapy utilizing PCI, it was decided to do an MTT assay for illumination times in the region from 0s to 210s (3 min) for detailed analysis.

The result of the MTT assay is presented in figure 9. The cell viability stayed unchanged from zero illumination until about 100s, where a rapid decrease occurred. At 120 seconds the viability of the cells had decreased to under 50% and at 165 seconds it reached a bottom line which stayed unchanged for all greater illumination times. The incubation time between illumination and MTT assay inspection was ∼70 hours. This lead to an increase in the number of viable cells in all samples which contained living cells after the PDT treatment. Therefore, the slope of the rapid decrease in viability present in figure 9, was presumably less steep 24 hours after illumination than presented here.

From these combined results, the PDT illumination protocol for HeLa cells was decided to contain illumination times of 30s, 60s, 75s, 90s, 105s and 120s. This protocol was used for all experiments with HeLa cells and chitosan vectors, as reported below.

4.3 PCI with Hela cells and linear chitosan/pDNA polyplexes

The experiment series with linear chitosan/pDNA polyplexes was done twice independent of each other. The only difference between the two experiments was the incubation time between cells were seeded and addition of photosensitizer. In the first series the incubation time was 5 hours, in the second it was about 24 hours. The polyplexes were prepared with an A/P ratio of 5.

4.3.1 Flow cytometry analysis

Figure 10 shows an overlay histogram representation for three different samples from the first experiment series: no treatment (blue), complexes (red) and PCI75 (green, 75s of illumination). The no treatment and complexes histograms are almost identical, the only difference being the complexes sample having a minor distribution broadening into the EGFP positive region of the graph. The PCI75 histogram also overlaps with the two other samples, but

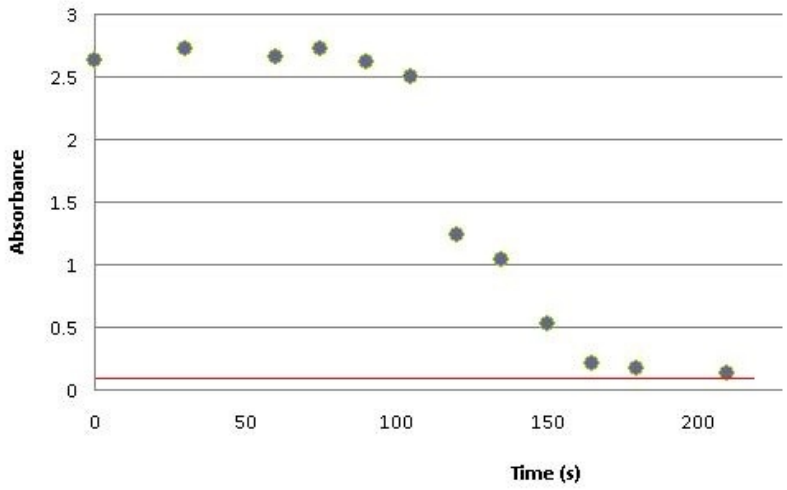

Figure 9: MTT absorbance curve as a measure of viability of HeLa cells after PCI treatment (absorbance in arbitrary units versus illumination times of PDT sample). The solid red line represents the average absorption in negative control samples containing no cells. All data points are averages of 4 samples (standard deviations within the data point symbols).

has significantly broadened distribution into the EGFP-positive region of the x-axis, showing that the transfection clearly has increased as a result of the PCI treatment (see figures 11 and 12 for transfection rates as a function illumination time for experiment series 1 and 2 respectively). The arithmetic mean value of the fluorescence intensity of the PCI sample was 79.7, whereas the others had arithmetic means at 2.1 (complexes) and 0.43 (no treatment). This is equivalent with almost a 40-fold increase in rate of transfection from the complexes to the PCI sample. All three histograms were gated on viable (PI negative) singlet cells.

Figures 11 and 12 shows graphs of survival rate for PDT, survival rate for PCI (both based on PI fluorescence) and transfection rate for PCI for the first and the second experiment series respectively. The transfection rate is given as the number of EGFP positive cells to the number of viable singlets in the sample.

For both experiment series the rate of transfection increased significantly from the control samples to the PCI samples which received 120s of illumination. The transfection rates increased from 1.00% and 0.56% to 49.8%

and 36.5% for series 1 and 2 respectively. This confirms that PCI enhances transfection of linear chitosan/pDNA polyplexes quite drastically.

Figure 13 gives the arithmetic mean EGFP fluorescence intensities of the EGFP positive cells versus illumination time for both living and dead cells treated with polyplexes of linear chitosan or SBTCO42. Looking at the graph for the living population treated with linear chitosan polyplexes (blue line), it is clear that the arithmetic means do not change significantly as the light doses are increased, but are stable at values around 200. This means that with increasing illumination time, only the number of transfected cells increases, not the grade to which the cells are transfected.

The graphs for survival rate for PDT and survival rate for PCI differs quite much for both experiment series. The only difference between the PDT and PCI samples of the same light dose is the presence of pDNA polyplexes in the PCI samples. These samples have without exception a lower survival rate than the PDT samples. The difference for the negative control samples (0s illumination) were in the region of 15%, whereas this difference had increased to almost 50% for samples which received 120s of illumination. This tells us that the PCI treatment somehow is more toxic than the PDT treatment in these experiments.

To analyze this last observation, a histogram of EGFP fluorescence gated on only dead (PI positive) cells was generated (see figure 14). Data from the same PCI sample as in figure 10 (PCI75) was used. As for the histogram gated on viable cells, this histogram has a broad distribution into the EGFP positive area. The arithmetic mean of the histogram was 180 and the transfection rate was 40.9%. Also, returning to figure 13, this plot shows that for the population of dead cells, the arithmetic mean increases from 380 to 500 between illumination times of 0s and 60s, before it drops steadily down to 220 at the illumination of 120s. For all illumination times, the arithemtic mean EGFP fluorescence was higher for the dead populations than for the living populations.

4.3.2 MTT analysis

An MTT assay was only available for the first experiment series. The assay contained control and PDT samples. A graphic representation of the microplate readout is seen in figure 15. These results confirmed what was observed in the flow cytometry analysis; the PDT samples showed little or no increase in toxicity with increased illumination time. The control sam-

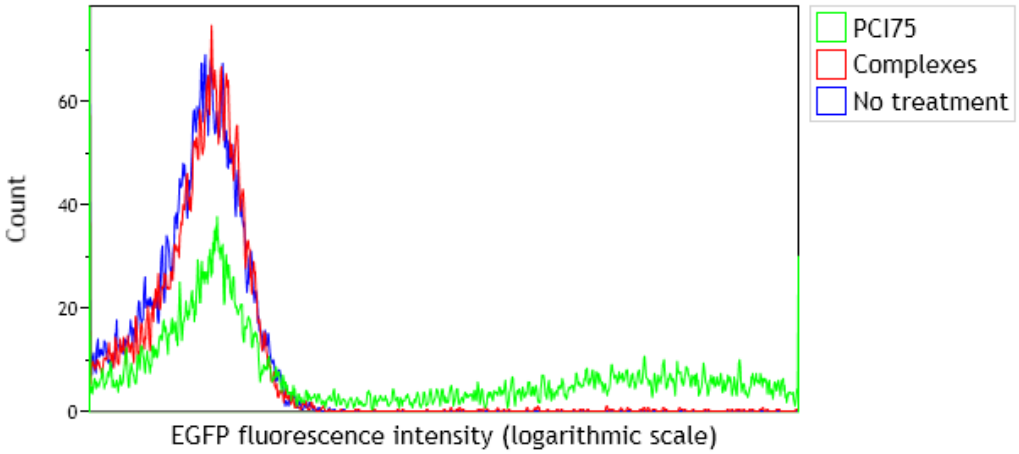

Figure 10: Overlay histogram of three different samples of HeLa cells with linear chitosan/pDNA polyplexes (counts versus EGFP fluorescence intensity): PCI75 (green), complexes (red) and no treatment (blue). The arithmetic means of the samples were: PCI75: 79.7, complexes: 2.1, and no treatment: 0.43. All histograms are gated on viable singlet cells.

ple containing complexes showed a toxicity comparable to the PDT samples, which stands in contrast to the FCM analysis where the toxicities of the complexes samples were greater than for the PDT samples.

4.4 PCI with HeLa cells and SBTCO/pDNA polyplexes

Experiments with two different SBTCOs were carried through, namely SBTCO42 and SBTCO31. SBTTO42 was prepared with an A/P ratio of 5, while SBTCO31 was prepared with an A/P ratio of 10. The protocol from section 3.2.2 was followed strictly for both experiment series and both experiment series were done once.

4.4.1 Flow cytometry analysis

SBTCO42 Figure 16 shows an overlay histogram for the no treatment, complexes and PCI60 samples. The histograms were gated on singlets, including both viable and dead cells (because of few cells in the samples). Both complexes and PCI60 samples have maxima overlapping with the PCI60 sample, but also broader distributions elongating into the EGFP positive region.

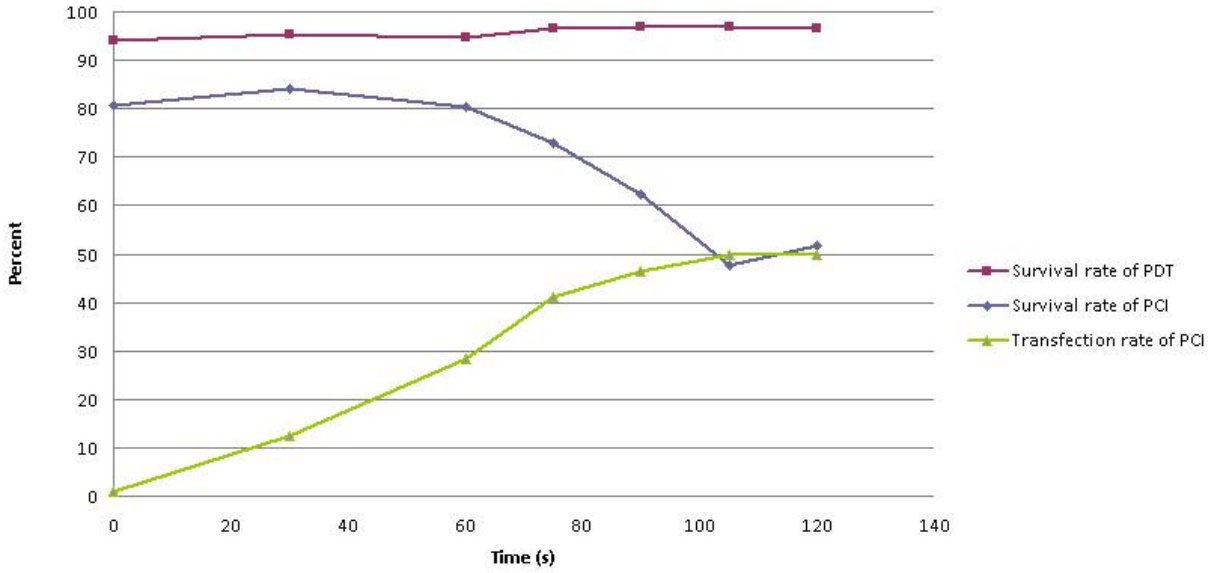

Figure 11: Graphs for survival rates after PDT and PCI treatment and transfection rates after PCI treatment for HeLa cells with linear chitosan/pDNA polyplexes, first experiment series (survival and transfection rates in percent versus illumination time). Transfection rates are percentages of living cells. All data points are averaged over two parallel samples.

The complexes sample also has a minor peak to the far right in the figure, indicating a population of cells which has high EGFP expression. The arithmetic means of the complexes sample was 119, whereas this was only 12.4 for the PCI60 sample.

Figure 18 shows the survival rate for PDT and PCI samples, as well as the rates of transfection for both viable and dead cells. Inspection of the figure reveals that an even greater difference in survival rate between PDT and PCI samples is present for the SBTCO42/pDNA polyplexes than was for the polyplexes of linear chitosan. The survival rate for PCI samples given zero illumination started at approximately 65% and immediately dropped to values as low as 20% and down to only a few percent as the light doses increased. The survival rate of samples treated with PDT on the other hand stays relatively stable at around 95% as the light doses are increased. The rate of transfection (gated on living cells) started at 17.4%, then increased to 42.1% after 60s of illumination, before it dropped down to under 10% and

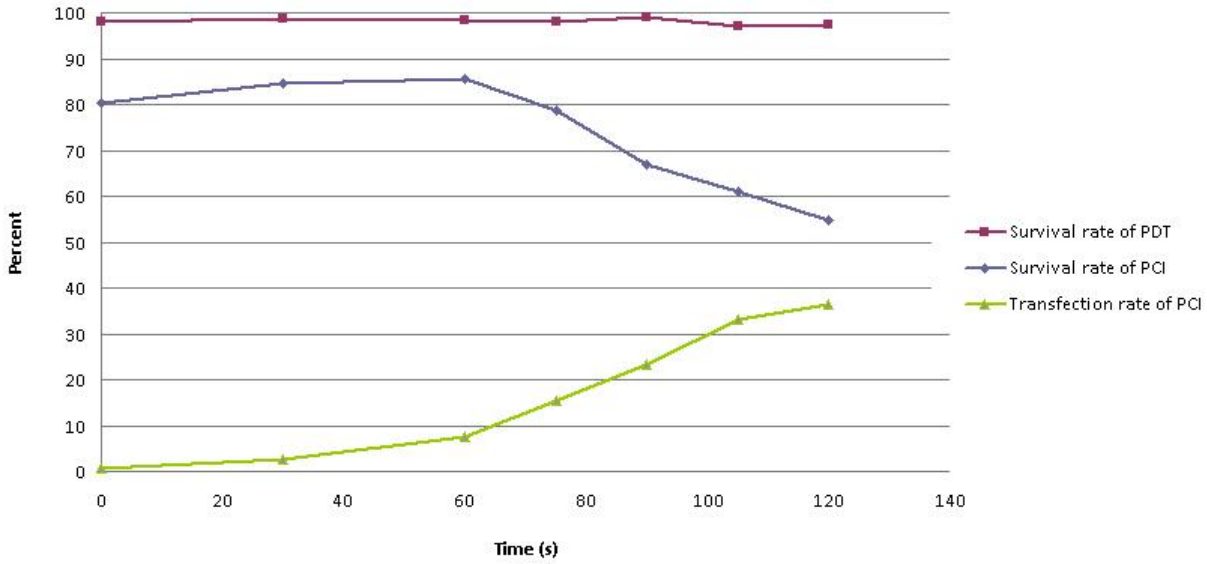

Figure 12: Graphs for survival rates after PDT and PCI treatment and transfection rates after PCI treatment for HeLa cells with linear chitosan/pDNA polyplexes, second experiment series (survival and transfection rates in percent versus illumination time). Transfection rates are percentages of living cells. All data points are averaged over two parallel samples.

ended at less than 5% after 120s of illumination. These transfection rates are not too reliable, since each PCI sample contained very few living cells (down to only some hundreds) to analyze the transfection rates from. The transfection rate of dead cells started at 48,2%, which was much higher than for the living cells. At light doses of 30s, the transfection rate had fell to ∼10%, and it continued down to ∼5% for light doses of 90s and more.

Returning to figure 13, the average arithmetic means of the positive living and dead populations can be studied. For the population of living cells, the arithmetic mean starts at ∼350 and decreases steadily until it reaches ∼150 at an illumination time of 90s (the data point for 120s was not available). For the population of dead cells, the arithmetic mean starts at a quite high value compared to the other populations, at ∼620. From here it decreases rapidly to ∼150 after 30s and 60s of illumination, and decreases further down to only ∼4 after 120s of illumination.

To see whether it was the batch of the SBTCO42 that induced the

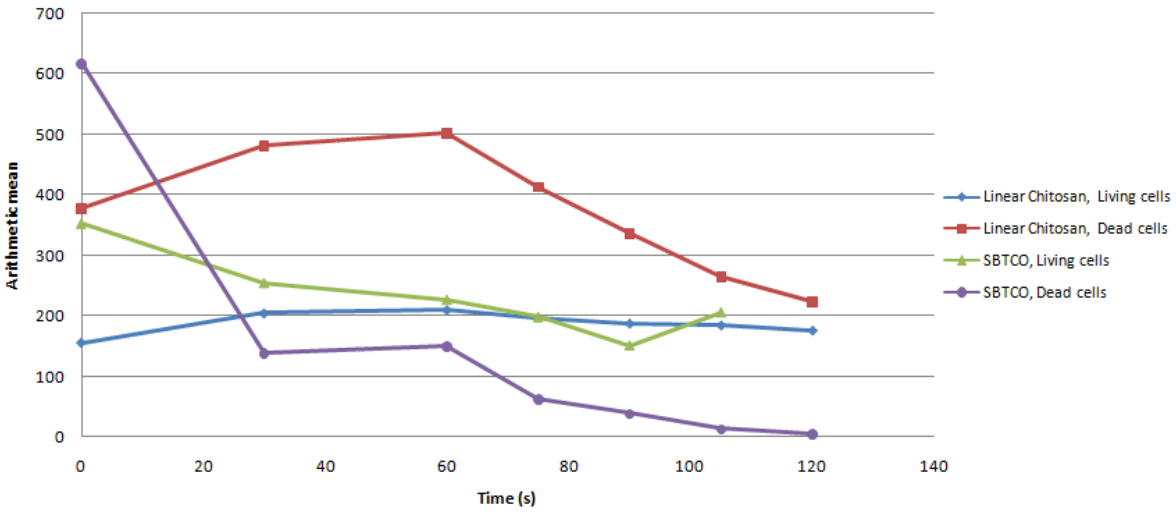

Figure 13: Graphs of average arithmetic mean of EGFP fluorescence intensity versus illumination time of the EGFP positive populations for polyplexes of linear chitosan and SBTCO. Individual plots are presented for the living and dead populations of linear chitosan (first experiment series) and SBTCO42. All data points are averaged over two parallel samples.

high toxicity observed, the next experiment series was carried through with SBTCO31 as transfection vector, which is very much alike the SBTCO42 vector, only differing slightly in molecular weights (SBTCO42: 27kDa, SBTCO31: 20kD).

SBTCO31 Results for the SBTCO31/pDNA polyplexes were quite comparable to those for the polyplexes of SBTCO42 (see figures 17 and 19). The overlay histogram (figure 17) revealed that the polyplexes were able to transfect the cells to a certain amount, and that this transfection was decreased as the PCI treatment was carried through (arithmetic means of 35.3 (complexes) and 24.7 (PCI75). No treatment: 0.46). The survival rate analysis revealed a drastic toxicity in all PCI samples as for the SBTCO42 polyplexes, and the uncertainty in the transfection rates were as great as before for the same reason (too few viable cells). The transfection rate in dead cells was also greater than for living cells in samples which received no illumination, following the same pattern as for the SBTCO42/pDNA polyplexes.

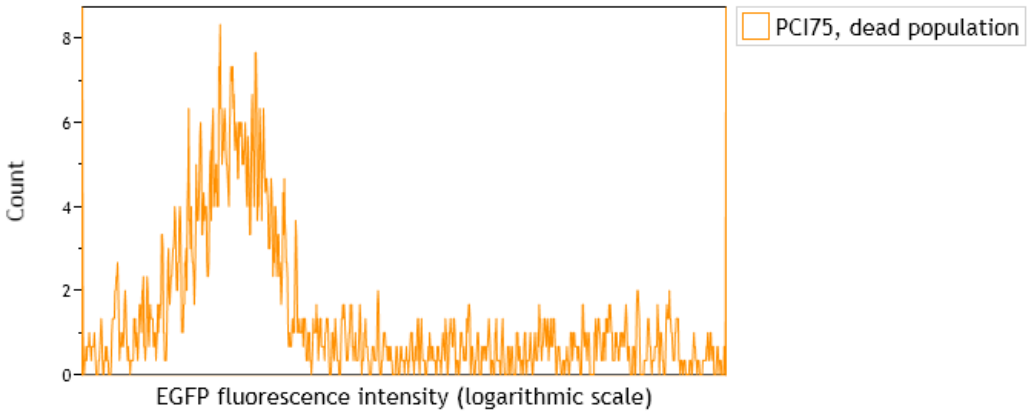

Figure 14: Histogram of a sample treated with PCI and 75s of illumination (linear chitosan polyplexes) gated on only dead singlet cells. The arithmetic mean of the sample was 180.

Included in this experiment were also samples containing uncomplexed SBTCO31 (pDNA volume replaced with water) and hypertonic optimum solution without pDNA and chitosan. The bare hypertonic optimum had an average survival rate of 92.8% and the uncomplexed chitosan had an average survival rate of 89.8%.

4.4.2 MTT analysis

MTT analysis for both SBTCO42 and SBTCO31 revealed the same toxicity from polyplexes as found during FCM analysis (see figure 20). The samples with polyplexes and no illumination gave an absorbance of ∼10% of the absorbance of the no treatment samples, while the PCI samples showed an absorbance of 1% to 5% of the no treatment level. The absorbance of the PCI samples were only slightly higher and even as low as the absorbance from the blank samples (100% DMSO).

As for the FCM analysis, the MTT setup for SBTCO31 also included samples of uncomplexed chitosan and bare hypertonic optiMEM. These samples both showed reduced absorbance compared to the PDT and no treatment samples. The absorbance relative to the no treatment level was at 28% for the bare hypertonic optiMEM sample and at 25% for the uncomplexed chitosan sample.

A uncomplexed pDNA sample was also prepared and inspected in the

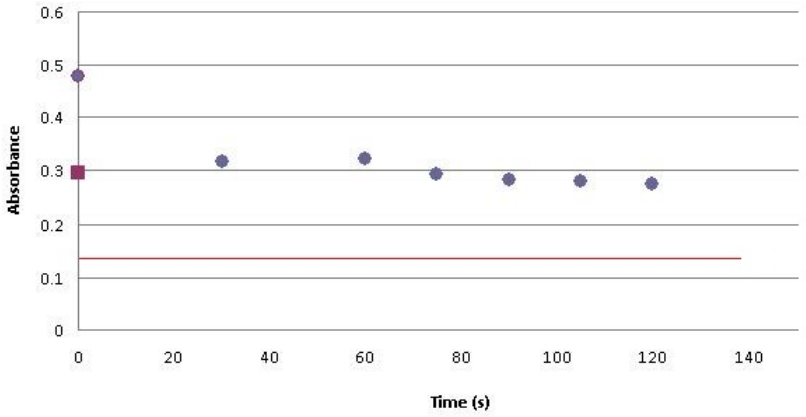

Figure 15: MTT absorbance curve as a measure of viability of HeLa cells after PDT treatment with polyplexes of linear chitosan (absorbance in arbitrary units versus illumination time). Circles: PDT samples, square: complexes sample (one control sample). The solid red line represents the average absorption in negative control samples containing no cells. All data points are averaged over three parallel samples (standard deviations within the data point symbols).

optical microscope. This sample did not show any significant reduction in survival (confluency) compared to a no treatment sample 24 hours after addition of pDNA. In contrast, a third sample in the setup containing polyplexes did show excessive cell death after 24 hours.

4.5 Comparison of toxicity of DNA plasmids

A final experiment was carried through with a EGFP DNA plasmid provided by Sabina Strand. This EGFP DNA plasmid had been used before without showing elevated toxic effects. When survival rates for samples containing polyplexes which had received no illumination were compared, polyplexes of both new and old plasmids gave excessive cell death (data not shown). The survival rates were found to be $\sim$50% and $\sim$65% for polyplexes of the new and old EGFP DNA plasmids respectively. Comparable absorbance values were also found for the samples using MTT analysis.

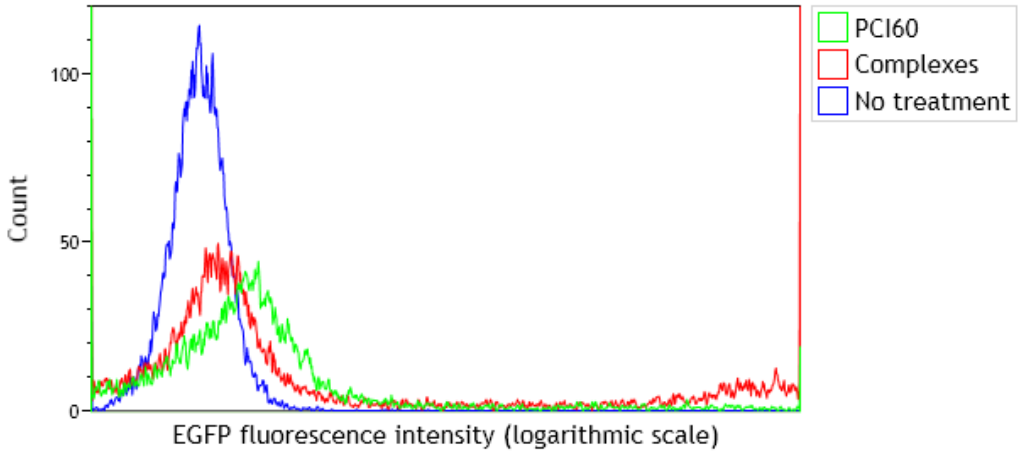

Figure 16: Overlay histogram of three different samples of HeLa cells with SBTCO42/pDNA polyplexes (counts versus EGFP fluorescence intensity): PCI60 (green), complexes (red) and no treatment (blue). The arithmetic means of the samples were: no treatment: 0.44, complexes: 119 and PCI60: 12.4.

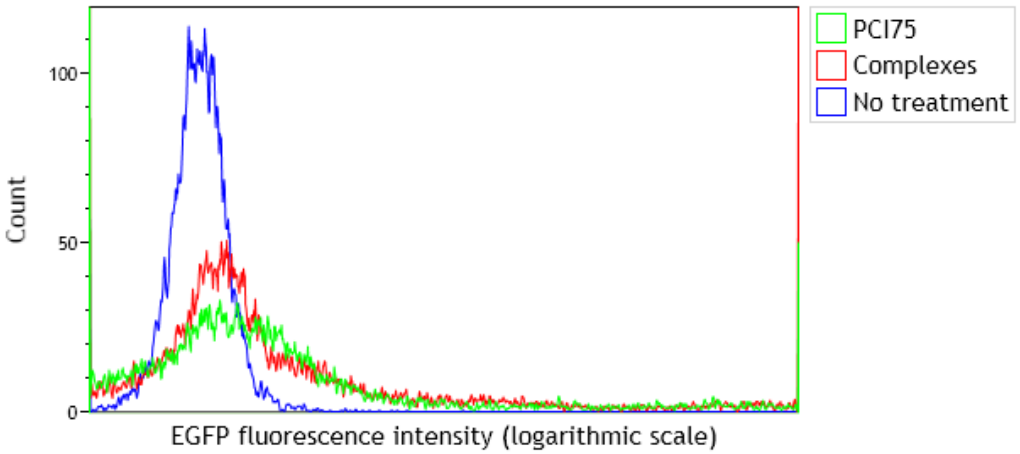

Figure 17: Overlay histogram of three different samples of HeLa cells with SBTCO31/pDNA polyplexes (counts versus EGFP fluorescence intensity): PCI75 (green), complexes (red) and no treatment (blue). The arithmetic means of the samples were: no treatment: 0.46, complexes: 35.3 and PCI75: 24.7.

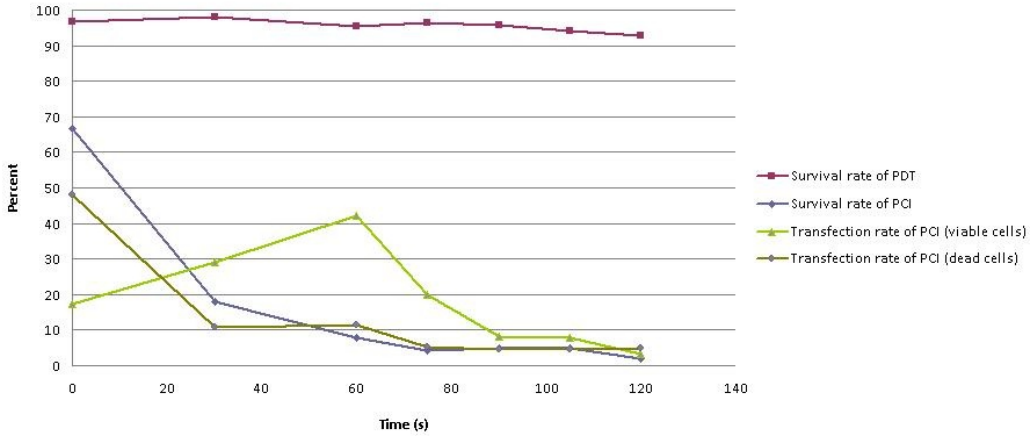

Figure 18: Graphs for survival rates after PDT and PCI treatment and transfection rates of both living and dead cells after PCI treatment for HeLa cells with SBTCO42/pDNA polyplexes (survival and transfection rates in percent versus illumination time). Transfection rates are percentages of living cells. All data points are averaged over two parallel samples.

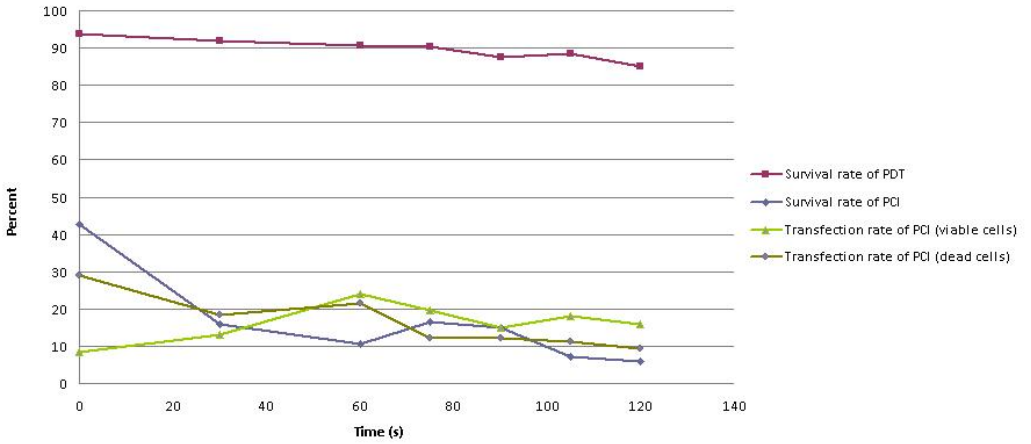

Figure 19: Graphs for survival rates after PDT and PCI treatment and transfection rates of both living and dead cells after PCI treatment for HeLa cells with SBTCO31/pDNA polyplexes (survival and transfection rates in percent versus illumination time). Transfection rates are percentages of living cells. All data points are averaged over two parallel samples.

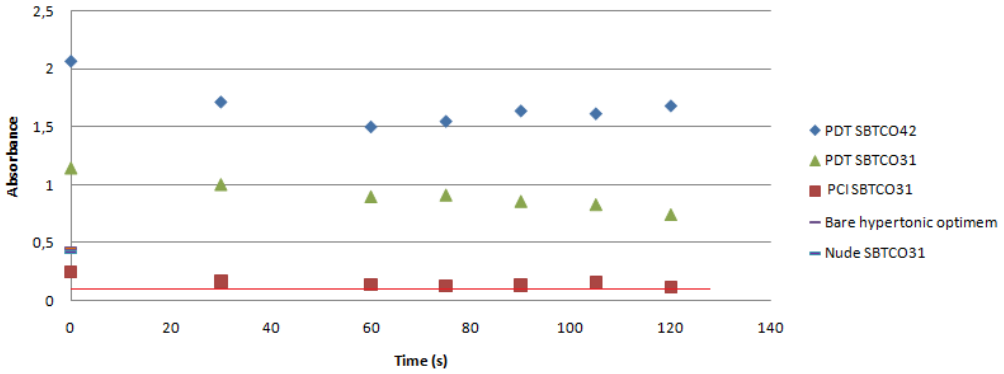

Figure 20: MTT absorbance curves as a measure of viability of HeLa cells after PDT and PCI treatment with polyplexes of SBTCO. Blue squares: PDT of SBTCO42, green triangles: PDT of SBTCO31, red squares: PCI of SBTCO31. The solid red line represents the average absorption in negative control samples containing no cells. Orange and blue marks on the y-axis represents the absorption from bare hypertonic optiMEM and uncomplexed chitosan (SBTCO31) respectively. The data are collected from two different experiment series. The PDT SBTCO42 data is from one series, whereas all the other data are from a second series. All data points are averaged over three parallel samples (standard deviations within the data point symbols).

5 Discussion

5.1 Methods and protocols

5.1.1 Light spill during experiments

None of the experiment series had any significant decrease in survival rate (FCM) or viability (MTT) in the no light samples (containing photosensitizer) compared to the no treatment samples (<5% difference). This reveals good laboratory practice and working environments where spilling of light to the samples were avoided to a high extent.

5.1.2 Incubation time before MTT analysis

When initially analyzing the toxic effects of the $TPCS_{2a}$ photosensitizer when illuminated in HeLa cells, the incubation time between illumination and inspection was 24 hours for the initial inspection with optical microscope and 72 hours for the MTT analysis (see figure 9). This difference is probably evident in the results. The inspection done 24 hours after illumination showed a clear gradient in cell density from 100% to 5% as the illumination time increased from 0s to 120s.

For the MTT analysis where the incubation time was 72 hours, the viability kept constant until a sharp break occurred between light doses of 105s and 120s. Since the cells were incubated three times as long as for the microscopy inspection, where the toxic effects also were clearly visible, the cells had time to divide several times before analysis by the MTT assay. This would give an increase in confluency of all samples which contained viable cells after illumination, resulting in several samples reaching the maximal amount of cells possible (given by the effect of contact inhibition) as present in the samples of 0s illumination. As a conclusion, a more smooth transition from viable to non-viable cell samples would be more probable to reflect reality than the sharp transition present in figure 9.

5.1.3 Incubation time for settling of cells

The first and second experiment series with HeLa cells and linear chitosan/pDNA polyplexes had different incubation times between seeding of cells and addition of photosensitizer (5 and 24 hours respectively). When analyzing the results from the first series the absorbance values from the MTT assay were

quite low, less than 0.5 after 3 hours of incubation in MTT solution. The absorbance values for the toxicity analysis previously done had reached values up to 2.5.

When analyzing the second experiment series, the absorbance values after 4.5 hours of incubation in MTT solution was up to 4, which is the saturation value of the microplate reader. This indicates that the incubation time for attachment of cells is critical regarding the initial cell concentration in the sample. Far more cells will have had time to settle after 24 hours of incubation than after 5 hours. When incubating for as long as 24 hours, many cells will also have had time to divide once or several times, resulting in a further increase in initial cell concentration.

The difference in cell concentration was also seen in the FCM analysis. All samples in the first experiment series which received PCI treatment with high light doses had a very low cell count. This was not a problem in the second experiment series. Also, the rate of transfection and toxicity of PCI samples reached higher values in the first experiment series than in the second (see figures 11 and 12). Since the samples of the first experiment series had a lower cell concentration than the samples of the second series, this would result in a higher number of both polyplexes and photosensitizer per cell in each sample, which could explain the higher transfection rates and toxicities observed.

5.1.4 Survival rate analysis versus viability analysis

In many of the experiment series, differences between survival rates from FCM analysis and viabilities from MTT assays were present.

The MTT assay is an indirect method of estimating the relative amount of living cells in a sample. Since the method relies on metabolic activity, a reduction in the cells' metabolism would give decreased production of farmazan salt and therefore also decreased absorption, even though the amount of cells in the sample did not change. A sample which on the other hand experiences toxicity such that a portion of the cells die, but otherwise do not suffer from decreased metabolism, will also give reduced absorbance when analyzed with the MTT assay. By this, these samples will give the same result when analyzed, even though the amounts of living cells not are the same in the two samples.

The survival rate analysis in FCM depends on the cells having permeable plasma membranes to allow PI to diffuse into the cell nucleus. This is

a characteristic of early apoptotic and apoptotic cells. By this, the size of the PI positive population is an estimate of the amount of dead cells in the sample.

Both the PI and the MTT methods give indirect measures of the toxicity in a sample, only estimating the real value. Since the methods evaluate different properties of the cells, metabolism for MTT analysis and plasma membrane permeability for the FCM analysis, differences can occur even though the toxicities in comparable samples in reality are the same.

5.2 Cellular transfection and uptake mechanisms

5.2.1 Transfection after PCI treatment

Both linear chitosans and SBTCOs are established transfection vectors for gene delivery. When mixed in solution with pDNA they self assemble to nano particles in the suitable size range for cell transfection (∼100nm), because of their polycationic properties [19]. Polyplexes of linear chitosan are not able to transfect cells to a higher extent than a few percent, whereas the SBTCOs being tailored specifically for transfection purposes have shown to give transfection rates up to 70% in HeLa cells (Sabina Strand et al., unpublished results).

When given PCI treatment, polyplexes of both types of chitosan did give increased rates of transfection. For the linear chitosan polyplexes, the effect of PCI was quite dramatic, giving an increase in transfection rate from ∼1% up to 50%, which is a 50-fold increase. This was done twice in independent experiments, and the outcome was the same both times. The effect of PCI was also evident for the two SBTCO chitosans. The rate of transfection was more than doubled for polyplexes of both SBTCOs from illumination times of 0s to 60s (17% to 42% for SBTCO42 and 8% to 24% for SBTCO31).

The increased transfection after PCI treatment revealed in this study for both types of chitosan vectors confirms that the bottleneck of transfection of cells using chitosan/pDNA polyplexes is the endosomal release. PCI treatment does not affect the uptake of polyplexes into endocytic vesicles, only the release from these vesicles is enhanced by the technique. The increased transfection achieved with PCI treatment indicates that chitosan polyplexes are taken up abundantly by the cells, but are never released from the endocytic vesicles before they are destined for the caveosome or the early endosome/lysosome (dependent on the pathway of uptake).

The transfection rates achieved for polyplexes of SBTCOs in this study did not reached the highest levels obtained in some earlier studies (70%). Nevertheless, the transfection rates did increase more than 2-fold as a result of the PCI treatment, clearly demonstrating that the treatment had a significant effect.

For light doses of 75s and above, the transfection rates of SBTCO polyplexes decreased to levels comparable to and lower than transfection rates achieved without PCI treatment. For data points at illumination times of 60s and below, the total cell count per data point was reasonably high, 1000 to 2000 cells or more. The data points for illumination times of 75s and above had on the other hand all less than 200 cells per data point (except the PCI75 SBTCO31 polyplexes sample which contained $\sim$1500 cells). These numbers are very low, and can hardly be used in any reliable analysis. Nevertheless, the transfection rates did decrease for illumination times of 75s and more for both SBTCOs.

The cells treated with polyplexes of linear chitosan did not show such low cell count as the polyplexes of SBTCO, and the results are quite reliable for all data points.

5.2.2 Cellular uptake mechanisms

Several studies have suggested that the main uptake mechanisms for polycationic polyplexes are clathrin-dependent and caveolin-dependent endocytosis [11, 36]. Many polyplexes are found to be taken up through both pathways, whereas others mainly rely on one. In the latter case, transfection can significantly be reduced by inhibiting the dominant pathway [12].

The uptake mechanisms for both polyplexes of linear chitosans and SBTCOs have been analyzed through inhibition studies (unpublished results, Sabina Strand et al.). For linear chitosan/pDNA polyplexes both clathrin-dependent endocytosis and caveolin-dependent endocytosis were found to be of importance. For the SBTCO/pDNA polyplexes, caveolin inhibition resulted in a almost 100% decrease in transfection, giving this as the by far most important pathway for SBTCO/pDNA uptake. When considering that the PCI treatment did increase transfection using the SBTCO/pDNA polyplexes, it is possible to conclude that PCI treatment also does affect macromolecules taken up through the caveolin-dependent pathway. The results strongly suggests that PCI treatment enhances release from vesicles from this pathway, as well as for vesicless of the clathrin-dependent pathway,

which already is more established [26].

5.2.3 Fate of polyplexes after uptake

The fate of the chitosan/pDNA polyplexes after uptake depends on the pathway they are taken up through. If not released from the endocytic vesicles, the clathrin-dependent pathway transports the polyplexes to the early endosome, whereas the cavolin-dependent pathway transports the polyplexes to the caveosome [13]. The early endosome mature to an endosome, which then fuses with a lysosome. The lysosome contains numerous digestive enzymes which degrade the polyplexes if not released before this stage. The faith of the caveosome is on the other hand highly discussed, where fusing with the early endosome, the ER or the golgi complex are all proposed opportunities [13, 37]. This leads to uncertainty regarding where polyplexes taken up through the caveolin-dependent pathway ends inside the cell if not released from the vesicles during an early stage.

Another difference for polyplexes taken up through the different pathways is the pH level within the organelle they are taken up to. The pH of the caveosome is at physiological level (pH at 7.4), whereas the pH in the early endosome is reduced to $\sim$4.5. A question following from this is whether the activity of the photosensitizer used depends on pH. The cytotoxic efficacy of $TPCS_{2a}$ upon light exposure is not well known. However, $TPCS_{2a}$ is structurally similar to $TPPS_{2a}$, which have been studied to a higher extent. The fluorescence emission spectrum of $TPPS_{2a}$ does not change in the physiological pH range (pH 6 to 8), but decreases at pH $<$6 in an aqueous environment, which indicates aggregation of the photosensitizer. When, on the other hand, the photosensitizer is absorbed in a vesicle membrane, it will not have the opportunity to aggregate and the reduction in fluorescence emission is likely not occur [38, 39]. By this, it is reasonable to believe that both the activity and the concentration (since both types of vesicles bulges of the plasma membrane) of both the $TPPS_{2a}$ and the $TPCS_{2a}$ photosensitizer are equal in endocytic vesicles from clathrin- and caveolin-dependent endocytosis.

5.3 Cytotoxicity evaluation

The goal in gene therapy is to stably transfect and express a gene because of a desired property of the gene product, without inducing high toxicity in the host cell through the transfection method (this is of course not the case

if the gene product itself is cytotoxic and intended to induce apoptosis in the cell).

5.3.1 Observed cytotoxicity

When setting up the PCI protocol for the experiments, only the cytotoxic effect of the PDT treatment (that is photochemical damage) was evaluated. The result was a treatment protocol including illumination times up to values which induced 50% toxicity in HeLa cells. In all four experiment series done with chitosan/pDNA polyplexes, the survival rate was never below 85% for any of the PDT samples. These were survival rates much higher than expected from the toxicity analysis done, but were also very satisfactory levels compared to the transfection rates achieved. The linear chitosan/pDNA polyplexes were able to transfect up to 50% of the cells without introducing more than 5% toxicity caused by photochemical damage. This is comparable to and even better than what has been achieved in studies of PLL/EGFP in HCT116 cells [40].

Analysis with FCM and PI staining revealed high toxicity in PCI samples of long illumination times for linear chitosan/pDNA polyplexes and for all illumination times for SBTCO/pDNA polyplexes. For the linear chitosan/pDNA polyplexes the toxicity reached 50% at 120s of illumination, whereas the toxicity of SBTCO/pDNA polyplexes reached values of >90% for illumination times of 75s and longer. This toxicity could not mainly be caused by photochemical damage since the PDT treatment did not give elevated toxicity.

The cells in samples with massive cell death (>50%) were studied using a transmission light microscope (data not shown). The cells had reduced size and were contracted to a more spherical form compared to the stretched out form of non-dividing, viable HeLa cells. The surfaces of the cells were rough and uneven and fragments of cells were present to a high extent. A number of dead cells were floating around in the culture medium.

5.3.2 Mechanisms giving cytotoxicity

To analyze which factors which contributed to the observed toxicity, samples of uncomplexed chitosan, uncomplexed pDNA and bare hypertonic optiMEM

(1:2 dilution of optiMEM with water) analyzed using FCM and MTT (uncomplexed pDNA only inspected in light microscope). Neither resulted in elevated toxicity through FCM analysis, whereas both uncomplexed chitosan and bare hypertonic optiMEM showed reduced viability in MTT analysis (respectively 25% and 28% viable). Inspection of the uncomplexed pDNA sample did not reveal any significant difference from a no treatment sample. The cells were also tested for mycoplasma infection, which could have caused the cells to be highly sensitive to cytotoxic reagents. The test turned out negative. These combined results suggested that the induced toxicity of the PCI treatment had to be caused directly by the polyplexes, by the EGFP protein or by effects linked to these.

The EGFP protein has been reported to have a cytotoxic effect in cytosol [33].It is also known that the presence of chitosan stabilizes the EGFP protein in cytosol, which when using chitosan vectors would prolong the toxic effect of EGFP (Sabina Strand et al., unpublished results). If EGFP solely was the cause of the toxicity observed, it would be expected to see high transfection rates in the populations of dead cells. This was, however, not observed (see figures 18 and 19). The transfection rates of the dead populations of samples which did not receive light treatment were quite high, ∼50% and ∼30% for SBTCO42 and SBTCO31 polyplexes respectively, but these rates decreased rapidly with increasing illumination.

It is also a possibility that the polyplexes induces cytotoxicity when present in high numbers in cytosol. The significant difference in toxicity of samples of linear chitosan/pDNA polyplexes and SBTCO/pDNA polyplexes without illumination (toxicities of ∼20% and ∼50%) could support this statement. The only difference between these samples is the chitosan vector, which in the latter case gave much higher transfection and therefore higher concentration of polyplexes in cytosol after 48 hours of incubation.

The relative toxicity of transfection with SBTCO/pDNA as a function of cell density in the samples was studied in one experiment by Sabina Strand (data not shown). This was done to investigate whether the high toxicity observed could be due to relatively low cell density (65.000 cells/mL) used in the described experiments compared to earlier experiments done with chitosan/pDNA. It was found that decreasing cell concentration did increase toxicity, likely because of increased polyplex concentration. The observed toxicity did however not reach the values reported here.

5.3.3 Effect of elevated cytotoxicity

The precise cause of the elevated toxicity remains unclear, thus it is likely that a combination of the reasons discussed led to the massive cell death observed. Analyzing the plots in figures 18 and 19 gives further information about the dead cells. For the dead cells treated with polyplexes of SBTCOs, the transfection rates are high for both types of polyplexes (SBTCO42 and SBTCO31) at 0s of illumination, but decreases rapidly as the illumination time increases. This pattern was also seen for the linear chitosan polyplexes where the transfection rate of dead cells started to decrease after 75s of illumination (data not shown). Data of the arithmetic means of the EGFP positive populations can be seen in figure 13. For the dead populations, the arithmetic means of the cells decrease as the illumination time increases. These results can possibly be explained by diffusion of EGFP protein out of the cells after the cells died.

The inspection by optical microscopy of the high toxicity samples revealed that much cell debris were present and that the morphology of the cells had changed drastically. The dead cells would in this case have leaky and permeable membranes, letting PI diffuse into the cell to stain nuclear DNA. Also, if the membranes were permeable enough, they would let EGFP protein diffuse out of the cell.

The effect of PCI treatment is an effective up regulation of the rate of release from endocytic vesicles. This would lead to a sudden and drastic increase of polyplexes in cytosol which further would give elevated EGFP expression which possibly could be too much for the cells to handle, leading to death through apoptosis. A natural effect following apoptosis is permeable plasma membranes, allowing EGFP protein to diffuse out of the cell. If this process of diffusion is simple and only depends on time, the earlier the cell died before FCM analysis was done, the more EGFP would have had time to diffuse out. If it assumed that higher light doses giving a more abrupt polyplex release and EGFP expression result in earlier cell death than for lower illumination times, this could give more diffusion of EGFP out of cells which received more light.

All this taken together can indicate that the cells treated with SBTCO/pDNA polyplexes and PCI were transfected to much higher rates at illumination times of 75s and higher than what was detected through FCM analysis.

5.4 Future perspectives

The technique of PCI is established as a reliable and effective technique for inducing cytotoxicity in mammalian cells *in vivo* in combination with a chemotherapeutic agent [26]. PCI has also proved capable of enhancing both specificity and transfection rates in gene therapy [41], as also confirmed by data presented in this study. Chitosan/pDNA nanoparticles have been studied intensively over the last years. Several studies have also reported that polyplexes of these types have been able to effectively transfect mammalian cells both *in vitro* and *in vivo* [2, 42].

Utilizing the technique of PCI in combination with chitosan/pDNA nanoparticles can hopefully in the future contribute to highly specific and effective gene therapy. The advantage of using PCI is the technique's capability of site-specific action. Using linear chitosan/pDNA polyplexes, gene therapy of very high specificity can possibly be achieved, since these polyplexes only would be able transfect cells in areas which received light treatment. Areas which did not receive light treatment would not experience more than $\sim$1% transfection.

A general obstacle of *in vivo* gene therapy is effective distribution of gene complexes in the target tissue, resulting in large areas with too low gene complex concentration for effective transfection [40]. By using a gene vector with good transfection properties *in vitro* (as the SBTCOs) in combination with PCI, effective transfection can possibly be achieved despite the low polyplex concentration. This is, of course, if the problem of cytotoxicity observed in this study can be decreased to a reasonable level.

For *in vivo* applications of PCI in gene therapy, the toxic effect observed here and in other studies may be crucial, if the target tissue has to stay unharmed. This is however not always critical, and cell killing can in some cases (e.g. most cancer treatments) be beneficial, even though the toxic effect not mainly is the purpose of the gene therapy. For these purposes, the chitosan vectors used in this study could be good candidates.

5.5 Further work

To further investigate the effect of chitosan/pDNA polyplexes in combination with PCI, it would be beneficial to repeat the experiments of this study, in particular those of SBTCO/pDNA polyplexes, with samples of higher cell concentration, e.g. 100.000 cells/mL. Hopefully this would give higher

transfection rates for long illumination times also for the SBTCO/pDNA polyplexes, and also reduce the observed toxicities for these samples.

To investigate whether the EGFP protein did induce cytotoxicity, experiments could be carried out in parallel with polyplexes of the EGFP plasmid and polyplexes of a non-coding plasmid. If higher toxicities were found in the samples containing polyplexes of EGFP plasmids, this would indicate that the EGFP protein is cytotoxic in these experiments.

It would also be interesting to do experiments with lower polyplex and/or photosensitizer concentrations, to see whether this could give a more gradual (but still enhanced) release from the endocytic vesicles. This could possibly stress the cells less, giving less cell death, and thus also higher transfection rates.

6 Conclusion

This study combined gene therapy using chitosan/DNA nanoparticles with PCI. The effect of the PCI treatment was elevated transfection rates for both types of chitosan vectors studied. When using illumination times of 120s for polyplexes of the linear chitosan vector, the observed increase in transfection was quite drastic, going from ∼1% to ∼50%. Transfaction rates of SBTCO/pDNA polyplexes were more than doubled for illumination times of 60s compared to 0s of illumination. Together this strongly suggests that endosomal release is one of the big bottlenecks in *in vitro* cell transfection using chitosan/pDNA polyplexes.

SBTCO/pDNA polyplexes are almost entirely taken up by the cell through the cavolin-dependent pathway. The increased transfection of these polyplexes as a result of PCI treatment reveals that PCI also is effective for release from vesicles from the caveolin-dependent pathway/the caveosome.

PCI treatment with high illumination times lead to excessive cell death, especially for the SBTCO/pDNA polyplexes. This toxicity was not induced by photochemical damage, but rather caused by the polyplexes, the EGFP gene product or mechanisms linked to these. For most therapeutic applications, this toxic effect has to be decreased.

The results from this study generally showed that PCI in combination with chitosan/pDNA polyplexes is a promising technique for effective and cite specific-gene therapy.

References

[1] Thomas C.E., Ehrhardt A., Kay M.A. Progress and problems with the use of viral vectors for gene therapy. Nat Rev Genet, 4: 346-358, 2003.

[2] Zheng F., Shi X-W., Yang G-F., Gong L-L., Yuan H-Y., Cui Y-J., Wang Y., Du Y-M., Li Y. Chitosan nanoparticle as gene therapy vector via gastrointestinal mucosa administration: Results of an in vitro and in vivo study. Life Sciences, 80: 388-396, 2007.

[3] Berg k., Folini M., Prasmickaite L., Selbo P.K., Bonsted A., Engesæter B.Ø., Zaffaroni N., Weyergang A., Dietze A., Mælandsmo G.M., Wagner E., Norum O-J., Høget A. Photochemical Internalization: A New Tool for Drug Delivery. Current Pharmaceutical Biotechnology, 8: 362-372,2006.

[4] Definition of Gene Therapy from The Medical Dictionary webpage. `http://medical-dictionary.com/`

[5] Douglas K.L. Review paper. Toward Development of Artificial Viruses for Gene Therapy: A Comparative Evaluation of Viral and Non-Viral Transfection. Biotechnol. Prog., 24: 871 - 883, 2008.

[6] Mulligan R.C. Review paper. The basic science of gene therapy. Science, 260, 926-932, 1993

[7] The Reuters webpage covering the death caused by viral gene therapy: `http://www.reuters.com/article/idUSBNG29636920070726`

[8] Genetics Home Reference. Schematic overview of gene therapy by a viral vector. `http://ghr.nlm.nih.gov/handbook/therapy?show=all`

[9] Pichon C., Billiet L., Midoux P. Chemical vectors for gene delivery: uptake and intracellular trafficking. Current Opinion in Biotechnology, 21: 640-645, 2010.

[10] Schatzlein A.G. Non-viral vectors in cancer gene therapy: principles and progress. Anti-Cancer Drugs, 12: 275-304, 2001.

[11] Rejman J., Bragonzi A., Conese M. Role of Clathrin- and Caveolae-Mediated Endocytosis in Gene Transfer Mediated by Lipo- and Polyplexes. Molecular Therapy, 12: 468-474, 2005.

[12] Gabrielson N. P., Pack D. W. Efficient polyethylenimine-mediated gene delivery proceeds via a caveolar pathway in HeLa cells. Journal of Controlled Release, 136: 54-61, 2009.

[13] Mayor S., Pagano R. E. Review article. Pathways of clathrin-independent endocytosis. Molecular Cell Biology, 8: 603-612, 2007.

[14] Parton R. G.,Howes M. T. Revisiting caveolin trafficking: the end of the caveosome. The Journal of Cell Biology, 191: 439-441, 2010.

[15] Dumitriu S., Vårum K. M., Smidsrød O. Polysaccharides Second Edition, chapter 26: Structure-Property Relationship in Chitosans, Marcel Dekker, 2005.

[16] Lai W-F., Lin M. C-M. Nucleic acid delivery with chitosan and its derivatives. Journal of Controlled Release, 134: 158-168, 2009.

[17] Strand S.P, Lelu S., Davies D.dL., Artursson P., Vårum K.M. Molecular design of chitosan gene delivery systems with an optimized balance between polyplex stability and polyplex unpackind. Biomaterials, 31: 975-987, 2010.

[18] Picture found on German Wikipedia in the public domain. `http://de.wikipedia.org/wiki/Chitosan`

[19] Strand S.P., Danielsen S., Christensen B.E., Vårum K.M. Influence of Chitosan Structure on the Formation and Stability of DNA-Chitosan Polyelectrolyte Complexes. Biomacromolecules, 6: 3357-3366, 2005.

[20] Strand S.P., Issa M. M., Christensen B.E., Vårum K.M. Artusson P. Tailoring of Chitosans for Gene Delivery: Novel Self-Branched Glycosylated Chitosan Oligomers with Improved Functional Properties. Biomacromolecules, 9: 3268-3276, 2008.

[21] Issa M.M., Köping-Högård M., Tømmeraas K., Vårum K.M., Christensen B.E., Strand S.P., Artursson P. Targeted gene delivery with trisaccharide-substituted chitosan oligomers in vitro and after lung administration in vivo. Journal of Controlled Release, 115: 103-112, 2006.

[22] Dougherty T.J.,. Gomer C.J., Henderson B.W., Jori G., Kessel D., Korbelik M., Moan J., Peng Q. Review article. Photodynamic Therapy. Journal of the National Cancer Institute, 90: 889-905, 1998.

[23] Raab O. The effect of fluorescent agents on infusoria (in German). Z. Biol., 39: 524-526, 1900.

[24] Malik R., Manocha A., Suresh D.K. Photodynamic therapy - A strategic review. Indian Journal of Dental Research, 22: 285-291, 2010.

[25] Berg K., Selbo P.K., Weyergang A., Dietze A, Prasmickaite L., Bonsted A., Engesæter B.Ø., Angell-Petersen E., Warloe T., Frandsen N., Høgset A. Porphyrin-related photosensitizers for cancer imaging and therapeutic applications. Juranl of Microscopy, 218: 133-147, 2005.

[26] Norum O-J., Selbo P.K., Weyergang A., Giercksky K-E., Berg K. Photochemical Internalization (PCI) in cancer therapy: From bench towards bedside medicine. Journal of Photochemistry and Photobiology, 96: 83-92, 2009.

[27] Lilletvedt M., Kristensen S., Tønnesen H.H., Høgset A., Nardo L. Time-domain evaluation of drug-solvent interactions of the photosensitizers $TPCS_{2a}$ and $TPPS_{2a}$ as part of physicochemical characterization. Journal of Photochemistry and Photobiology A: Chemistry, 214: 40-47, 2010.

[28] Mosmann T. Rapid Colorimetric Assay for Cellular Growth and Survival: Application to Proliferation and Cytotoxicity Assays. Journal oflmmunologicalMethods, 65: 55-63, 1983.

[29] Lecoeur H. Review article. Nuclear Apoptosis Detection by Flow Cytometry: Influence of Endogenous Endonucleases. Experimental Cell Research, 277: 1-14, 2002.

[30] The Green Fluorescent Protein. Tsien R.Y. Annual Review of Biochemistry, 67: 509-44, 1998.

[31] Shimomura O., Johnson F.H., Saiga Y. Extraction, purification and properties of aequorin, a bioluminescent protein from the luminous hydromedusan, Aequorea. Journal of Cellular and Comparative Physiology, 59: 223-39, 1962.

[32] Zhang G., Gurtu V., Kain S.R. An Enhanced Green Fluorescent Protein Allows Sensitive Detection of Gene Transfer in Mammalian Cells. Biochemical and Biophysical Research Communications, 227: 707-711, 1996.

[33] Liu H-S., Jan M-S., Chou C-K, Chen P-H., Ke N-J. Is Green Fluorescent Protein Toxic to the Living Cells? Biochemical and Biophysical Research Communications, 260: 712-717, 1999.

[34] Prased P.N. Introduction to Biophotonics, chapter 11: Flow cytometry. Wiley-Interscience, 2003.

[35] Open Wet Ware. Schematic representation of flow cytometry. Open Wet Ware has adopted the figure from: Givan A.L. Flow Cytomtry, Second Edition. Wiley-Liss, 2001. http://openwetware.org/wiki/BE.109:DNA_engineering/FACS_analysis

[36] Luhmann T., Rimann M., Bittermann A.G., Hall H. Cellular Uptake and Intracellular Pathways of PLL-g-PEG-DNA Nanoparticles. Bioconjugate Chemistry, 19: 1907-1916, 2008.

[37] Pelkmans L., Kartenbeck J., Helenius A. Caveolar endocytosis of simian virus 40 reveals a new two-step vesicular-transport pathway to the ER. Nature Cell Biology, 3: 473-483, 2001.

[38] Cunderlikova B., Bjorklund E.G, Pettersen E.O., Moan J. pH-Dependent Spectral Properties of HpIX, TPPS2a, mTHPP and mTHPC. Photochemistry and Photobiology, 74: 246-252, 2001.

[39] Cunderlikova B., Kaalhus O., Cunderlik R., Mateasik A., Moan J., Kongshaug M. pH-Dependent Modifcation of Lipophilicity of Porphyrin-type Photosensitizers. Photochemistry and Photobiology, 79: 242-247, 2004.

[40] Høgset A., Prasmickaite L., Marit Hellum M., Engesæter B.Ø., Olsen V.M., Tjelle T.E., Wheeler C.J., Berg K. Photochemical Transfection: A Technology for Efficient Light-Directed Gene Delivery. Somatic Cell and Molecular Genetics, 27: 97-113, 2002.

[41] Høgset A., Prasmickaite L., Selbo P.K., Hellumb M., Engesæter B.Ø., Bonsted A., Berg K. Photochemical internalisation in drug and gene delivery. Advanced Drug Delivery Reviews, 56: 95-115, 2004.

[42] Wong K., Sun G., Zhang X., Dai H.,Liu Y., He C., Leong K.W. PEI-g-chitosan, a Novel Gene Delivery System with Transfection Efficiency

Comparable to Polyethylenimine in Vitro and after Liver Administration in Vivo. Bioconjugate Chemistry, 17: 152-158,2006.

A Protocol for EGFP plasmid preparation

Growth of the bacterial culture The protocol is valid using the NucleoBond Xtra Midi kit[1] from Macherey-Nagel.

1. Remove competent cells[2] from -80°C and place directly on ice. Thaw cells for 5 to 10 min.
2. Gently mix cells by tapping tube.
3. Add 1-50 ng (or more) of DNA[3] into 100 μL competent cells. Gently tap tube to mix.
4. Place the tubes on ice for 20-30 min
5. Heat-shock the cells for 45 sec in a 42°C water bath or a heating block. Do not shake. Place the tubes on ice for 5 min.
6. Add 450 μL pre-heated LB medium to each transformation reaction.
7. Incubate at 37°C for one hour, with shaking (225-250 rpm).
8. Add 100 μl of the bacterial solution and spread on LB agar plates[4] containing appropriate antibiotic (e.g. 50 μg/mL kanamycin). Leave the plates with the agar-side down for minimum one hour. Turn the plates with the agar-side up before overnight incubation.
9. Incubate the plates at 37°C overnight (12 to 16 hours).
10. Pick a single colony from a freshly streaked agar plate. Inoculate a 2 ml starter culture of LB medium containing 50 μg/ml kanamycin[5] (or the appropriate selective antibiotic to guarantee plasmid propagation).
11. Incubate at 37°C for $\sim$8 h (or overnight) with shaking ($\sim$250 rpm)
12. Add 1 mL of the bacterial suspension into 125 ml preheated LB medium containing 50 μg/ml kanamycin (125 μl from stock 50mg/ml)

    or

13. Add 1 ml of the bacterial suspension into 1 ml 50% glycerol solution (final glycerol concentration should be 15-30%), and store at -80 until preparation of overnight culture.

14. Grow the culture overnight at 37°C and ∼200 rpm.

15. Add ∼40 ml of the overnight culture in three 50 ml tubes, and pellet the cells at 4500-6000 x g for 5-10 minutes.

16. Remove the supernatant. Leave the tubes upside down on a piece of paper to remove the rest of the supernatant.

17. Resuspend the cell pellet completely in resuspension buffer RES + RNase A1 by pipetting the cells up and down. Add 8 ml of buffer RES in the first tube. When resuspended, add the cells to the second tube, and mix thoroughly. Repeat the step for the third tube.

18. Add 8 ml lysis buffer LYS1 to the suspension. Mix gently by inverting the tube 5 times. (Do not vortex). Incubate for 5 minutes at room temperature. (It is important that the incubation time does not exceed 5 minutes to avoid the release of genomic DNA)

19. Equilibrate a column together with the inserted column filter with 12 ml equilibration buffer EQU1. Apply the buffer onto the rim of the column filter. Make sure to wet the entire filter.

20. Add 8 ml neutralization buffer NEU1 to the suspension and mix the lysate gently by inverting the tube 10-15 times.

21. Load the lysate onto the column. Allow the column to empty by gravity flow.

22. Wash the column filter and column with 5 ml equilibration buffer EQU1.

23. Discard the column filter and wash the column with 8 ml washing buffer WASH1.

24. Elute the plasmid DNA with 5 ml elution buffer ELU1. Collect the eluate in a 50 ml centrifuge tube.

25. Add 3.5 ml room-temperature isopropanol to precipitate the eluated plasmid DNA. Vortex well and let the mixture sit for 2 minutes.

26. Remove the plunger from a 30 ml syringe and attach a NucleoBond Finalizer[6] to the outlet. Fill the precipitation mixture into the syringe, insert the plunger and press the mixture slowly through the filter. Discard the flow-through.

27. Remove the Finalizer from the syringe, pull out the plunger and reattach the Finalizer to the syringe outlet. Fill 2 ml 70% ethanol into the syringe, insert the plunger and press the ethanol slowly through the filter. Discard the ethanol.

28. Remove the Finalizer from the syringe, pull out the plunger and reattach the Finalizer. Press air through the filter to dry the filter membrane. Repeat three times.

29. Remove the Finalizer from the syringe, pull out the plunger of a 1 ml syringe and attach the Finalizer to the syringe outlet. Pipette 600 μl redissolving buffer TRIS or TE into the syringe. Place the Finalizer outlet over an Eppendorf tube and elute the plasmid DNA carefully by inserting the plunger.

30. Remove the Finalizer from the syringe, pull out the plunger and reattach the Finalizer to the syringe outlet. Transfer the first eluate back into the syringe and eluate into the same tube a second time.

31. Use an UV spectroscopy, ex Gene Quant, to determine plasmid yield. Dilute the plasmid 1:100. Set the reference with 100 μl water in the cuvette.

32. Run the sample, and measure A_{260}, A_{280} and ratio. Run two parallels of each sample.

33. Confirm the plasmid integrity by agarose gel electrophoresis. 0,8-1,0 g agarose[7] is dissolved in 50 ml 1 x TBE with 5 μl SYBR Safe DNA gel stain[8].

34. Heat the agarose in a microwave oven for 20-30 seconds, until the agarose is completely dissolved.

35. Fill the chamber with the warm agarose, and leave it to dry for 30-60 minutes.

36. Add 8 μl of 2-log DNA Ladder[9] to the first well.

37. Mix 1 μl 6x DNA loading buffer[10] with 5 μl plasmid DNA (volume ratio 1:6) and add to the next well. The amount of DNA per well should be $\sim$1 μg.

38. Start the electrophoresis using 120 V. Make sure the DNA is migrating towards the anode.

39. Image the gel by using the Bio-Rad GelDoc[11] or another gel documentation system.

Suppliers

1. NucleoBond Xtra Midi, Macherey-Nagel, Cat.No 740410.50
   http://www.mn-net.com/Products/NucleicAcidPurification/PlasmidDNA/NucleoBondXtra/tabid/1479/language/en-US/Default.aspx

2. JM109 Competent cells, AllianceBio, Cat.No. M208CC85
   http://www.alliancebio.com/Downloads/MBProtocols$%$20PDF/M208CC85$%$20JM109.pdf

3. pEGFP-N1, Clontech Laboratories (Palo Alto, CA), Cat.No. 6085-1
   http://www.pkclab.org/PKC/vector/pEGFPN1.pdf

4. LB agar plates Kanamycin-50, Sigma-Aldrich, Cat.No. L0543
   http://www.sigmaaldrich.com/catalog/ProductDetail.do?lang=en&N4=L0543|SIGMA&N5=SEARCH_CONCAT_PNO|BRAND_KEY&F=SPEC

5. Kanamycin, Sigma-Aldrich, Cat.No. K4000
   http://www.sigmaaldrich.com/catalog/ProductDetail.do?lang=en&N4=K4000|SIAL&N5=SEARCH_CONCAT_PNO|BRAND_KEY&F=SPEC

6. NucleoBond Finalizer Plus, AH diagnostics, Cat.No. M740520.20
   http://www.mn-net.com/Products/NucleicAcidPurification/PlasmidDNA/NucleoBondFinalizerFinalizerLarge/tabid/1451/language/en-US/Default.aspx

7. TopVision Agarose, Fermentas, Cat.No. R0491
   http://www.fermentas.de/product_info.php?info=p1530

8. SYBR Safe DNA gel stain, Invitrogen, Cat.No. S33102
   http://products.invitrogen.com/ivgn/product/S33102?ICID=search-product

9. 2-log DNA Ladder, New England BioLabs, Cat.no N3200
   http://www.neb.com/nebecomm/products_intl/productN3200.asp

10. 6 x DNA loading buffer: 30% glycerol in ddH2O, 0.25% Bromophenolblue (BB) and 0.25% Xylene cyanol FF (XC)

11. GelDoc, Bio-Rad
    http://www.bio-rad.com/cmc_upload/Literature/72907/MI1708062BB_G.pdf

B Selected flowpages

A selection of different flowpages is presented below, as examples on how different results can look like.

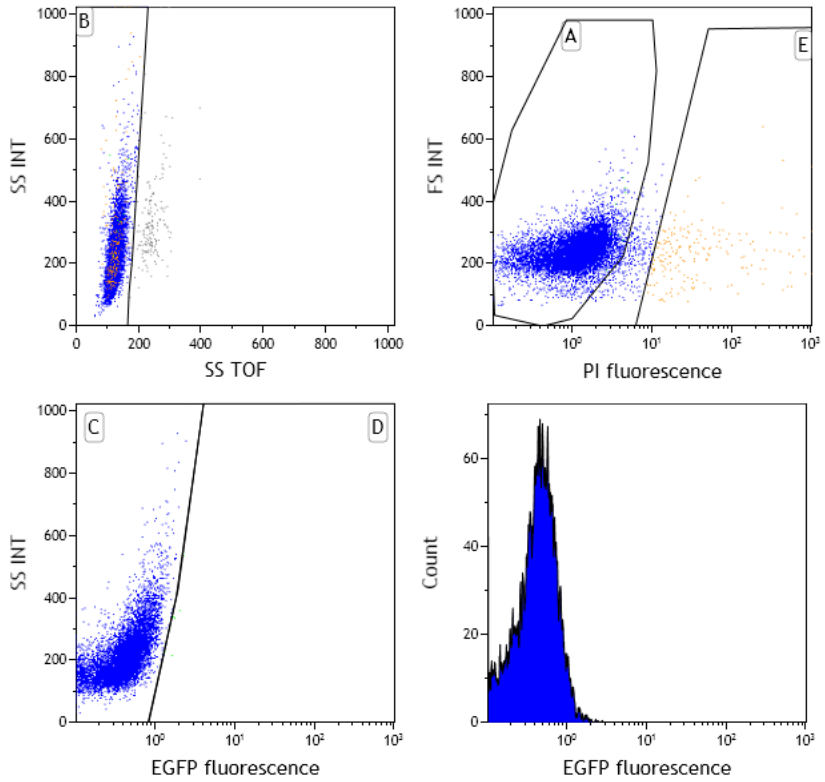

Figure 21: Flow page for a no treatment sample. Singlets are gated in the upper left figure (area B). Singlets are devided into living (area A) and dead (area E) populations in the upper right figure. The living EGFP negative cells (area C) are devided from the living EGFP positive cells (area D) in the lower left figure.

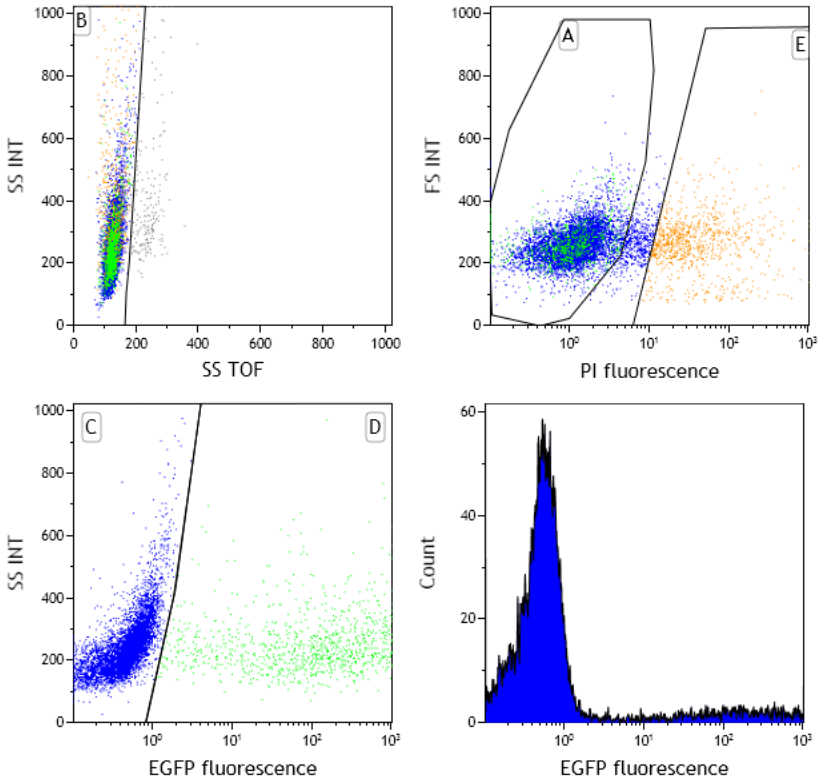

Figure 22: Flow page for a PCI30 sample of linear chitosan polyplexes. Singlets are gated in the upper left figure (area B). Singlets are divided into living (area A) and dead (area E) populations in the upper right figure. The living EGFP negative cells (area C) are divided from the living EGFP positive cells (area D) in the lower left figure.

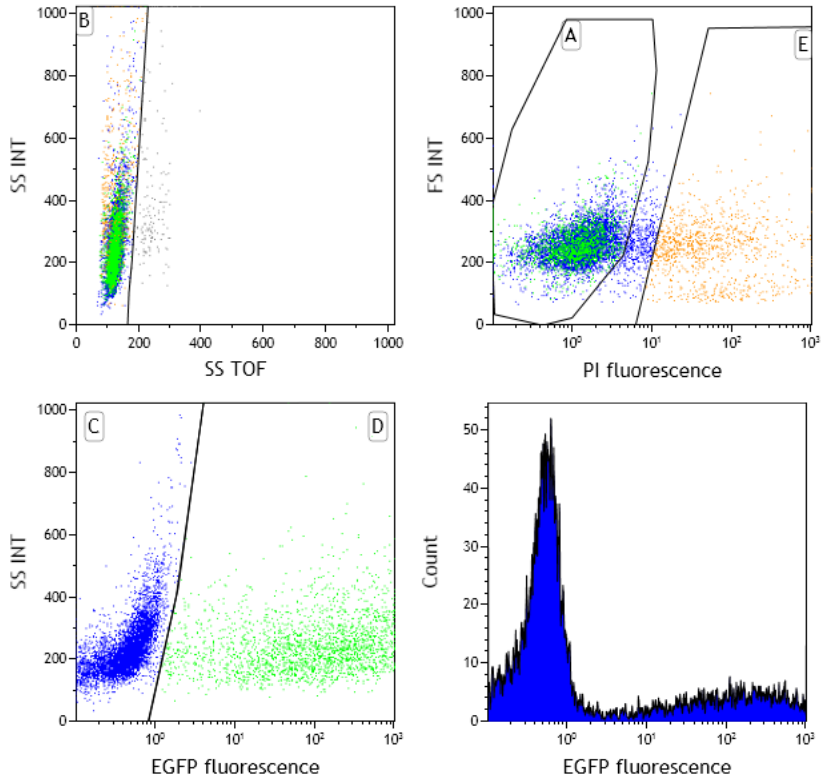

Figure 23: Flow page for a PCI60 sample of linear chitosan polyplexes. Singlets are gated in the upper left figure (area B). Singlets are divided into living (area A) and dead (area E) populations in the upper right figure. The living EGFP negative cells (area C) are divided from the living EGFP positive cells (area D) in the lower left figure.

C Compensation examples

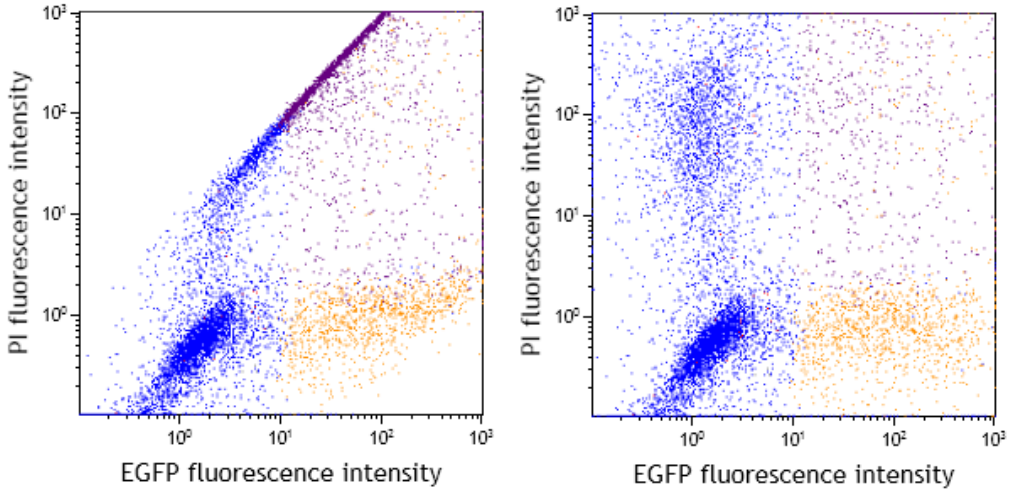

Figure 24: Dot plot of EGFP versus PI fluorescence without and with compensation. Left: The cells of high EGFP fluorescence intensity have also been detected in the PI detector and are therefore gated as dead cells. The pronounced line going from lower left to upper right is characteristic for uncompensated data. Right: The EGFP positive cells which earlier were detected by the PI detector are now placed directly above the rest of the PI negative cells.